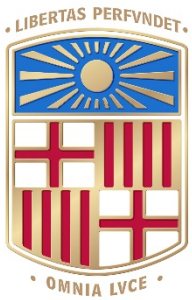

UNIVERSITAT DE BARCELONA

Final Degree Project

Biomedical Engineering Degree

"Design of a hydrogel-based microfluidic chip for Organ-on-Chip applications "

Barcelona, 6th of June 2022
Author: Marta Falcó Fusté
Director/s: María García Díaz and Núria Torras Andrés
Tutor: María García Díaz and Núria Torras Andrés

Acknowledgments

First of all, I would like to express my sincere gratitude to my directors and tutors, María García Díaz and Núria Torras Andrés for their patience, support and trust throughout the duration of the project and to Dr Elena Martínez for giving me the opportunity to do this project in her group, whose members have made me feel very welcomed.

Secondly, I would like to extend my gratitude to Oscar Castillo for his knowledge and help throughout the project.

Finally, and on a more personal note, I would want to say thank you to my family and friends for their unconditional support.

Abstract

Organ-on-chip is an emerging technology that combines microfluidic devices with 3D cell cultures to provide *in vitro* models that resemble the *in vivo* physiology of organs and tissues. These platforms can be used to understand the dysfunctions and pathogenesis of the body and to perform drug development and toxicology assays. Since in colorectal cancer the survival rate is very low when metastasis has occurred, the development of technologies that can be used to test new drugs and improve the prognosis of the disease is essential. Organ-on-chip can be used to model the tumor vascular microenvironment and provide a platform to understand the metastatic process by means of a vessel-on-chip, which would simulate the blood-vessel environment. However, current vessel-on-chip devices lack the translational capability to clinical outcomes. Therefore, in this project we aim to design, fabricate and validate a hydrogel-based microfluidic chip for *in vitro* modelling a blood vessel by embedding fibroblasts in the gel to recreate the surrounding extracellular matrix and support the later endothelial cell seeding in its walls. On the one hand, hot embossing technique was used to fabricate PMMA substrates of the chips. Screws and nuts were used to seal the devices to avoid the mixture of fluids in the outlets of the different channels and leakage. On the other hand, SLA 3D bioprinting approach was used to fabricate GelMA-PEGDA hydrogels that sustained the encapsulated fibroblasts. Different chip geometries were designed and validated including cell-laden hydrogels under flow conditions. Live/Dead™ assay was performed to assess cell viability of the encapsulated fibroblasts at different time points. Results shown that over 50% of the cells were alive after 7 days in culture in the chips, proving its feasibility, yet attributed to the lack of medium flow in the channels due to leakage. Even though further improvements are needed, this microfluidic device can be obtained using precise, low-cost and fast fabrication techniques and has offered promising results in terms of cell viability.

Keywords: Organ-on-chip / vessel-on-chip / microfluidic device / 3D bioprinting / hydrogels

List of contents

1. Introduction

It is widely known that the cellular microenvironment plays a vital role in cellular morphology and the activation of factors that regulate cell growth, proliferation and differentiation [1]. Therefore, over the last decades, efforts have been focused on developing cell culture platforms that consider cell-environment interactions since traditional cell culture methods, such as culture plates and Petri dishes, fail to replicate them [2]. For that purpose, conventional two-dimensional (2D) cell cultures are being replaced by three-dimensional (3D) cell cultures, to generate more realistic *in vitro* models. In a 3D cell culture, an artificial cellular microenvironment is created with a biological scaffold or matrix that emulates the extracellular matrix (ECM) and mechanically supports cell growth [2]. This scaffold must be biocompatible to allow the growth, proliferation, differentiation, and migration of the embedded cells, providing access to oxygen and nutrients.

Extensive research has been performed to determine whether hydrogels are good candidates to act as ECM surrogates in tissue engineering. Hydrogels are 3D networks of polymer chains with highly tunable mechanical and chemical properties, which are also able to absorb large amounts of fluids because of their porous nature, which is relevant in the diffusion of oxygen and nutrients [3]. To resemble the ECM, hydrogels must possess a hydrated protein and a polysaccharide network which can be derived from either synthetic or natural polymers, or even from the combination of both. Unlike hydrogels from synthetic polymers, hydrogels from natural polymers, such as those composed by gelatin methacryloyl (GelMA), contain growth factors and integrin binding sites for promoting cellular functions, like cell attachment and proliferation. Nevertheless, both types of polymers maintain cell viability [2].

One of the most advanced technologies to produce biomimetic scaffolds for cell encapsulation is 3D bioprinting. There are different types of 3D printing technologies, yet their purpose is to develop a 3D volume by sequentially depositing or crosslinking a specific material, commonly named as ink, in a cross-sectional pattern [4]. The way in which the ink is deposited creating the printed volume is the main difference between the multiple existing bioprinting technologies. For instance, stereolithography (SLA) is a high-resolution light-based 3D bioprinting technique in which light coming from a focused laser or a digital-light processing (DLP) projector is used to polymerize a photocrosslinkable material layer by layer [5]. Consequently, the precursor solution (or ink) must contain a photoinitator, which will produce reactive species when exposed to light. Such species, named free radicals, will react with monomers (or oligomers) from the ink leading to the final 3D scaffold. This ink can contain cells (bioink) resulting in scaffold with embedded cells developed from 3D bioprinting. Hydrogels have been proved to be printable, leading to uniform 3D structures of hundreds of microns with high resolution and reproducibility [6]. This, together with their excellent cell-friendly properties, make hydrogels the most widely used materials for the bioprinting of 3D cell culture scaffolds.

Traditional 2D cell cultures but also 3D cultures are usually made in static conditions, where the dynamic physiological conditions of cells cannot be reproduced. In this context, microfluidic chips can be used to overcome this issue and thus, recreate the processes that occur in vivo [7]. Microfluidic devices consist of a pattern of microchannels that allow for the application and precise

control of different flow conditions at the microscale in a local manner, minimizing the experimental times, leading to feasible devices with reduced production costs (simple technology) [8]. The microchannels are linked to the macroenvironment by several apertures through which the fluid is injected and ejected by external pumps or pressure sources at controlled rates. Therefore, these devices in combination with 3D cell cultures offer promising platforms to create *in vitro* models of organs or physiological processes by simulating the *in vivo* environment found in tissues [9]. These platforms are known as organ-on-chip (OoC) devices which, through the combination of cell biology, engineering, and biomaterials technology, the microenvironment of the chips simulate that of the organs in terms of tissue interfaces and mechanical stimulation [7].

OoCs can provide a better understanding of the dysfunctions and pathogenesis of the body because of their ability to reproduce the physiology *in vivo* in a local manner, using reduced amounts of reagents and cells. Hence, they can be used in drug development and toxicology studies to pave the way for personalized medicine since patient-derived cells can be used to run these tests. A case example would be to improve the prognosis of patients with colorectal cancer metastasis since, while their 5-year survival rate is of 91% when the cancer is localized, this rate drops to 72% when the cancer has spread to the surrounding tissues or organs even when patients are diagnosed at an early stage of the disease. The rate is even worse (15%) when the cancer has spread to distant parts of the body [10]. A better understanding of the process by which a cancerous cell detaches from the primary tumor, goes into the bloodstream or the lymphatic system and forms a new tumor on another organ it is crucial [11]. On this circumstances, OoC platforms could be used to mimic the tumor vascular microenvironment of patients with colorectal cancer to test new therapeutic strategies and help monitoring the course of the disease [12].

Blood vessels are essential to flow blood throughout the body. The inner wall of a blood vessel, which is located at the lumen of the artery, consists of a layer of endothelial cells that are embedded in a 3D microenvironment that serves as ECM[13]. This ECM is mainly composed by proteoglycans and fibrous proteins such as collagen, fibronectin, elastin and laminin [13], which form the basal lamina, that separates the endothelial wall from the rest of the matrix, and the connective tissue, which also contains fibroblasts cells [14](Figure 1). Therefore, in this project we aim to develop a Vessel-on-Chip (VoC) that mimics a blood-vessel environment to eventually be used to understand metastasis and test new drugs.

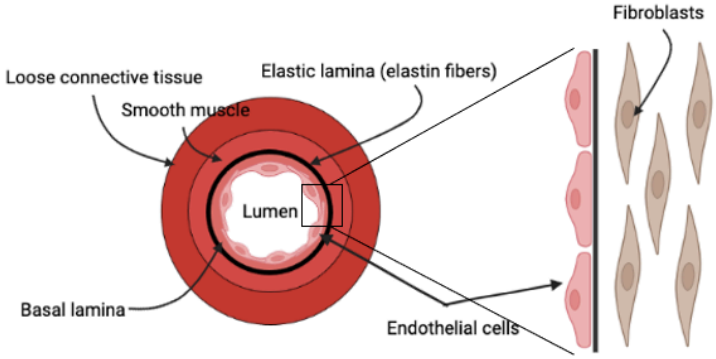

Figure 1: Schematic overview of a blood vessel and the endothelial cell microenvironment. Adapted from [68]. Created with biorender.com

1.1. Aim and scope of the project

The present project aims to fabricate and validate a microfluidic device for *in vitro* modelling of a blood vessel. The VoC will be a hydrogel-based microfluidic chip, in which the hydrogel will embed fibroblasts and support endothelial cell seeding in the walls to recapitulate the microenvironment of a blood vessel.

1.2. Objectives

The previously described goal is achieved through the following secondary objectives:

- To design the casing, also referred to as the external/outer part of the microfluidic chip containing the microchannels, to encase the printed hydrogel, avoiding fluid leakage and ensuring independent flows through the different channels.
- To design reusable two-channel and three-channel microfluidic chip using a fast and reproducible fabrication technology.
- To fabricate hydrogel scaffolds with SLA bioprinting, with and without embedded cells.
- To obtain an OoC and obtain high cell viability inside the chip.
- To seed endothelial cells to recapitulate a blood vessel microenvironment.

1.3. Methodology

This project has been developed at the Institute of Bioengineering of Catalonia (IBEC) in the Biomimetic Systems for Cell Engineering group leaded by Dr. Elena Martínez Fraíz, from February to June of 2022. It was carried out mostly by doing experimental research, together with a bibliographic review of the state of the art. Moreover, information regarding the previous work performed by the group was also considered to develop this model. The project has been divided into different stages:

a) Development of the outer part of the microfluidic chip, including a search for an appropriate biocompatible material that could be easily manipulated by using known microfabrication techniques, and sealed properly to avoid leakage.
b) Optimization of the microfluidic connections, set-up and flow conditions to guarantee proper microenvironment surrounding the hydrogel located inside the chip, while assuring proper media exchange.
c) Design hydrogel scaffolds (shape and dimensions) for their perfect fit into both two-channel and three-channel chips designs, after swelling.
d) 3D printing of hydrogels with embedded stromal cells (fibroblasts) to mimic the basal lamina of the blood vessels.
e) Assess cell viability of the embedded fibroblasts.
f) Seed endothelial cells
g) Model evaluation

2. Background of the project

The combination of 3D cell cultures, composed by cells and a biological scaffold, with microfluidic devices are aimed to increase the reliability of the models to mimic the human physiology.

2.1. Microfluidic devices for organ-on-chip

Microfluidics is a group of techniques that precisely manipulates and processes microscale fluids using channels whose size are in the range of microns [15]. These devices, commonly known as Lab-on-Chip (LoC) or Point-of-Care systems, allow fast reaction times, the use of small sample volumes and the induction of laminar flow, resulting in a more precise control of the processes [16]. The evolution of LoCs has led to the development of OoCs, whose main goal is to simulate the physiological environment of human organs by regulating concentration of gradients, shear forces, cell patterning, tissue boundaries and tissue-organ interactions [15]. Many scientific articles endorse the use of OoC to improve the relevance of cell studies. For instance, Qin *et al.* demonstrated that the hepatic spheroids cultured in a liver-on-chip based on hydrogel performed liver-specific functions of albumin/urea secretion and cytochrome P450 (CYP) expression than the corresponding static culture within 8 days resulting in an improved ability to mimic the liver microenvironment [17]. Sung and Shuler also showed that, while the cytotoxic effect of Tegafur, which is the oral product of an anti-cancer drug, was not seen in the culture of different cell types embedded in a 3D hydrogel (tumor cells, liver cells and myeloblasts) in a 96-well microtiter plate, when the same culture was set in a microfluidic device the toxicity of the drug could be quantified, emphasizing the relevance of these devices [18].

Since the development of microfluidic technology, many different materials have been explored using several types of technologies, such as milling, casting, replica, and injection molding, etc., always focusing on reproducibility and low-cost. The use of polymers has been extensively studied, giving special attention to polydimethylsiloxane (PDMS). PDMS microfluidic chips are mainly obtained through soft-lithography processes, which consists in transferring a pattern from a mold, obtained by photocuring a resin on top of a silicon wafer, to an elastomeric material like PDMS. In fact, a large portion of research papers published on microfluidic devices are using PDMS as main substrate material to build OoCs to model different organs [19, 20, 21].

Lee *et al.* developed a liver-on-chip with PDMS obtained through soft-lithography in which hepatic sinusoids were modeled using primary rat and human hepatocytes cultured in endothelial-like microfluidic channels [19]. In this design, the sinusoidal structure of the liver was recreated, and they used cell chambers, flow channels and endothelial barriers. Kilic *et al.* presented a brain-on-chip to model migration of human neural progenitors in response to chemotactic cues within the brain-tissue setting [20]. They developed a three-layer chip of PDMS to recapitulate the neural and vascular compartments in the brain, which are separated by the blood-brain barrier. The top and bottom compartments could be perfused as channels of 5 mm width, 20 mm length, and 300 μm height. The top compartment had around 100 support pillars distributed across the channel in a hexagonal array to prevent membrane collapse. They were separated by a 10 μm-thick PDMS membrane with 5 μm diameter holes. Finally, these PDMS chips were attached to glass coverslips to provide support and increase image resolution (see Figure 2). Other examples include bone marrow-on-chip to replicate the hematopoietic niche physiology *in vitro* providing a more relevant platform to perform drug toxicology studies [21]. The model was built in a PDMS chip containing a cylindrical central chamber that is separated from the underlying and overlying channels by porous membranes.

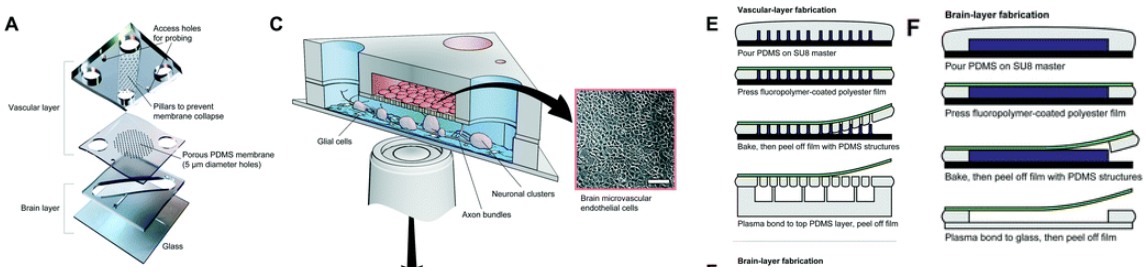

Figure 2: Structure and fabrication of brain-on-chip platform by Kilic *et al.* (A) Structure of device consisting of all-PDMS parts attached to glass. (C) Cross-section of final brain-on-chip platform showing a NGCP layer consisting of human neuronal and glial cells, interacting through a perforated membrane with a monolayer of human brain microvascular endothelial cells (scale bar = 250 µm). (E and F) Fabrication process of the devices. Adapted from [20].

PDMS has some advantages including elasticity which enables leakproof microfluidic connections as well as an easy integration of microvalves and micropumps, its biocompatibility, transparency, inertness, oxygen and gas permeability, low autofluorescence, tunable mechanical properties depending on its preparation (proportion, curing times and temperatures) and it is easy to activate and functionalize, making PDMS suitable for some biological applications. However, it has some disadvantages including the loss of mechanical properties over time, the release of molecules due to a bad crosslinking, the sensitivity to certain chemicals, or non-specific absorption of small molecules, among others [22]. Apart from these disadvantages, a critical step in using PDMS as substrate material for microfluidic chips is the sealing process to prevent leakage. One of the most common approaches refers to sealing the PDMS onto a glass slide by using oxygen plasma treatment, which activates the surfaces to join. This treatment removes the organic, hydrocarbon material by chemical reaction with highly reactive oxygen radicals and ablation by energetic oxygen ions. During this reaction SiOH groups are exposed and, when the two surfaces are put in contact, Si-O-Si bonds are formed releasing H_2O molecules. Campisi *et al.* used this methodology to develop a functional model of human blood-brain barrier with endothelial cells, pericytes and astrocytes to perform studies of the BBB barrier [23]. However, the union generated between the surfaces is unstable, meaning that fluid leaks can occur after some uses, which decreases the reliability of the models [23]. Moreover, plasma treatment requires the application of pressure and heat between the two contact surfaces to secure the bonding, limiting the fact that cells embedded in hydrogels could be placed inside the chip after the bonding.

In this context, the use of thermoplastic materials for OoC is increasing [24]. These materials can be remolded by reaching glass transition temperature and can retain the shape of templates after cooling, enabling its patterning [25]. The main technologies to manipulate thermoplastics are hot embossing and injection molding [8], which require expensive equipment that might not be available in standard labs, which can make these materials unsuitable for prototypic use. On the one hand, hot embossing set-up consists of an upper plate, in which a master or mold is attached, and a lower plate, which heats the polymer above its glass transition temperature. Then, a load is applied on the polymer through the upper plate and the pattern from the master is transferred to the polymer [26]. On the other hand, injection molding is the process of melting polymers until they are malleable enough to be injected at pressure in a mold cavity, in which the polymer will solidify and produce the final product [27].

Despite the high cost of the equipment and material required to apply these technologies, both of them have been explored using PMMA as OoC substate because of its chemical properties, low price, optic transparency, ease of fabrication, biocompatibility and excellent mechanical properties [28]. Nonetheless, polymethylmethacrylate (PMMA) also has certain disadvantages including low gas permeability and inflexibility. For example, Miller and Shuler designed a gravity-driven PMMA-based microfluidic chip that allowed high cell viability over 7 days of different cell lines and the maintenance of cellular functions like albumin release [29]. This Body-on-chip (BoC) consisted of different layers held together with stainless steel screws generating the channels and the different culture compartments as shown in Figure 3.

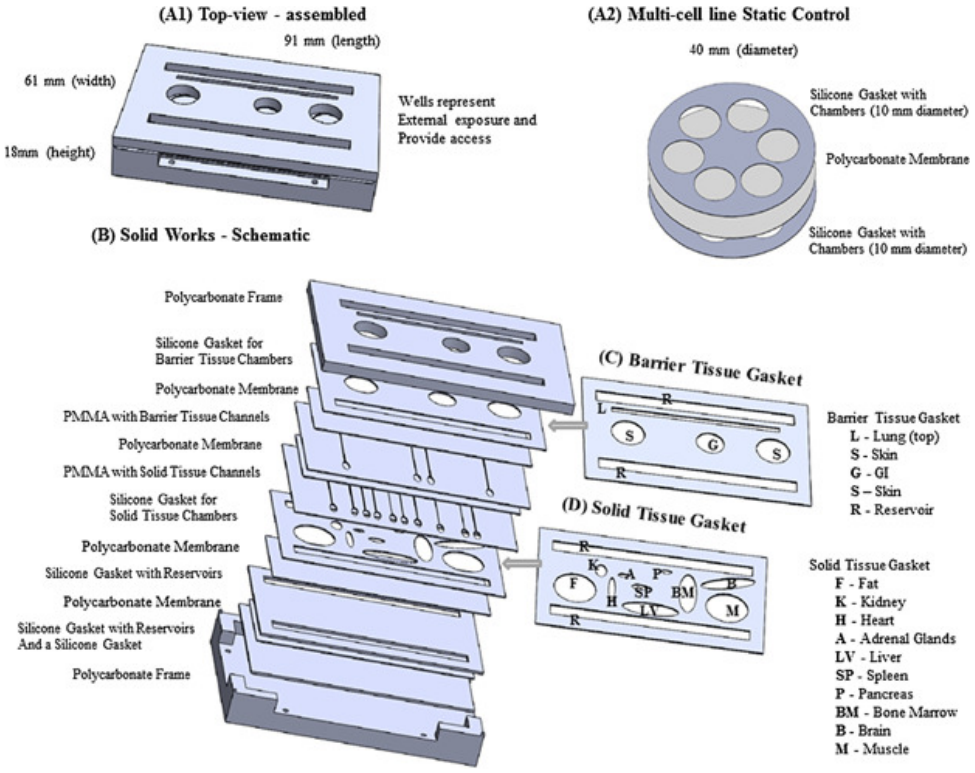

Figure 3: PMMA-based BoC that consists of layers held by stainless screws. From [29].

2.2. Hydrogel components

Conventional 2D cell culture has been a well-established and accepted technique to study cell behavior among the scientific community. However, the *in vivo* cell microenvironment is not properly represented and therefore, accurate models of diseases and studies of cell growth and proliferation cannot be achieved [30]. For example, Li *et al.* reported that human hepatocytes lose key phenotypic and hepatic characteristics in within 7 days when they are cultured as 2D monolayers, whereas by co-culturing hepatocytes with mesenchymal stem cells in a collagen scaffold, the function of the cells is preserved for 21-28 days [31]. Therefore, the development of technologies to generate biocompatible scaffolds to be used in 3D cultures has been essential to improve the biological model's accuracy and provide better biomimetic platforms with more physiological relevance and predictive capability than 2D cultures [30].

An increasingly popular choice regarding the materials to create 3D scaffolds are hydrogels, which are polymer networks able to imbibe large amounts of water. Their popularity relies on their well-

known biocompatibility and controllable physicochemical properties, that can be tuned with their composition. In general, hydrogels can derive from polymers of natural or synthetic origin, which can be combined to produce networks with a large variety of characteristics, as function of their final application. Some of the most common hydrogel materials are alginate, collagen, gelatin, fibrin, agarose, poly(ethylene) glycol (PEG) and derivates or polyacrylamide (PAA) [32].

The biomimetic systems for cell engineering group at IBEC has been developing hydrogel co-networks mainly based on the combination of photo-crosslinkable GelMA and PEGDA polymers to build 3D models that resemble the human extracellular microenvironment by means of light-based 3D bioprinting technology. The combination of both materials has shown good results for tissue engineering applications. PEGDA provides mechanical stability to the printed structures and GelMA offers good cellular response favoring their growth and attachment. These polymers are combined with the visible light lithium phenyl-2,4,6-trimethylbenzoylphosphinate (LAP) photoinitiator and an additional photoabsorbing agent known as tartrazine. On the one hand, LAP is essential to ensure the photopolymerization reaction required to build the 3D network in presence of light source, whereas the role of tartazine is to improve the resolution of the printing results, interacting with part of the irradiated light. Tartrazine is a synthetic azo dye highly soluble in water at low concentration, that has an absorption peak centered around 436 nm, overlapping the emission spectrum of the light source used for printing and being close to the LAP absorption peak (375 nm) [33].

Once printed, the properties of the resulting 3D hydrogel network will depend on the concentration of each component, but also on the printing parameters stablished (i.e. energy dose applied, the thickness and the exposure time per printed layer), and, in turn, these properties will determine the performance of the hydrogel for a specific application. These properties include the definition on the type of mesh and distribution, the quantification of pore size which determines the permeability and diffusivity, the study on the mechanical performance and the analysis on the physical and chemical stability including the degradation, remodeling, among others.

2.3. 3D bioprinting technologies

3D Bioprinting is defined as the spatial patterning of living cells and other biologic components such as growth factors by stacking and assembling them using a computer-aided layer by layer deposition technique for the fabrication of living tissue and organs [34]. This technology offers very precise spatial and temporal resolution to construct scaffolds of specific architectures while allowing for the control of porosity through the control of the printing parameters [35]. In tissue engineering, 3D bioprinting is used to print the scaffolds that will serve as ECM [3] using bioinks, which are the combination of biomaterial solution and one type (or more) of living cells.

There are four types of techniques widely used in bioprinting, namely:

a) **Inkjet-based bioprinting** which deposits drops of a specific bioink onto a substrate in a controlled manner. Drops are pushed through either mechanical, thermal or electromagnetic forces and hence, it is considered a no-contact printing technique. Despite being a fast and affordable technology, the precision is not as good as other types of bioprinting methods [3]. Zhang. *et al.* reported the use of inkjet printing to develop a 3D model in a microfluidic chip for drug studies. [36] They developed a self-made inkjet printing

system to print alginate scaffolds through the optimization of the parameters that controlled the ejection of the droplets. One of the most important parameters are claimed to be alginate concentration which determines the viscosity of the solution since sodium alginate is already a very viscous material, which difficult the controlled ejection of the bioink over other methods.

b) **Extrusion-based bioprinting** uses a syringe loaded with a bioink in which continuous pressure is applied to extrude the material while it moves along the printing bed [37]. However, cell viability can be jeopardized if the applied pressure or the viscosity of the bioink, to improve the control over the printing process, is very high. Wanjun *et al.* modified a commercial 3D printer to print hydrogels by coaxial extrusion [38]. They used a GelMA-Alginate bioink to print cell-laden hydrogels in which alginate was used to confine and serve as sheat for the GelMA to increase structural stability. Similarly, Gao *et al*. used coaxial extrusion bioprinting to develop 3D hydrogel-based vascular structures with multilevel fluidic channels, demonstrating the potential of this technology to simulate the *in vivo* vascular circulation [39].

c) **Laser-assisted bioprinting** uses the laser energy to photodegrade small focal volumes of polymer due to multiphoton absorption and generate scaffolds with a very precise architecture [34]. Hakobyan *et al.* demonstrated that this technology can be used to bioprint 3D pancreatic cell spheroid arrays with high control over cell number deposition and spatial resolution and that it can be used as an alternative to 2D cell cultures and other more time-consuming 3D approaches [40].

d) **Stereolithography (SLA)** uses light coming from either a projector (Digital Light Projection SLA or DLP-SLA) or a laser to pattern photocrosslinkable materials, that polymerize in presence of light. Since the polymerization occurs layer-by-layer, the resolution of the technique is high [41]. The laser-based approach requires larger fabrication times and full control of the energy dosage of the laser to prevent photoablation of the matrix and cell damage. Conversely, DLP-SLA bioprinting is faster and the resolution can be tunned with the concentration of the photoinitiators of the bioink. Zhang and Larsen reported the fabrication of SLA printed perfusion chips units where confined cell culture volume is traversed and surrounded by perfusable vascular-like networks [42]. In this study, the bioink was composed of PEGDA, LAP and a photoabsorber (quinoline yellow), and later functionalized with GelMA to accommodate live cells either forming a monolayer and/or embedded inside.

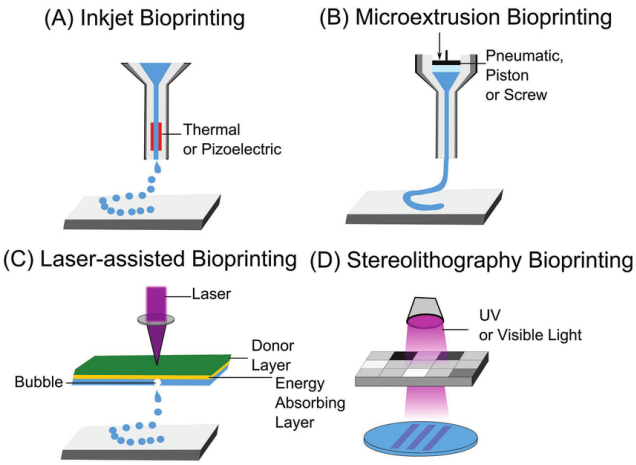

Figure 4: Four types of 3D Printing. From [69]

2.4. Vessel-on-chip

The dysfunction of the endothelial cells (ECs) that line in the lumen of blood vessels contributes to many diseases such as arteriosclerosis, stroke, cancer, and thrombosis. Therefore, to understand how microvasculature grow and remodel, it is essential to have reproducible systems that emulate the function of living tissues [43].

Two main strategies have been adopted so far for the fabrication of vessel-on-chip (VoC) systems [44]. The first one relies on the predesign of vascular channel networks within hydrogels, in which ECs are seeded later on top. Morgan *et al.* described a protocol to form 3D cell cultures with endothelialized microvessels on hydrogels [45]. To do it, they used a remodeled collagen-I hydrogel that was injected into a perfusable microfluidic device, to control mass transfer and hemodynamic forces. Soft-lithography was used to create a PDMS mold that was used to generate the collagen-based hydrogel scaffold with the tubular structures, later covered by endothelial cells. Similarly, Zhang *et al.* developed a thrombosis-on-chip model by means of sacrificial bioprinting [46]. They used Pluronic® to generate a 3D sacrificial scaffold that was placed on top of a PDMS support serving as a mold. The mold was then filled with GelMA prepolymer solution and UV crosslinked. Finally, the sacrificial structure was dissolved generating hollow channels later seeded with ECs to model blood vessels (see Figure 5).

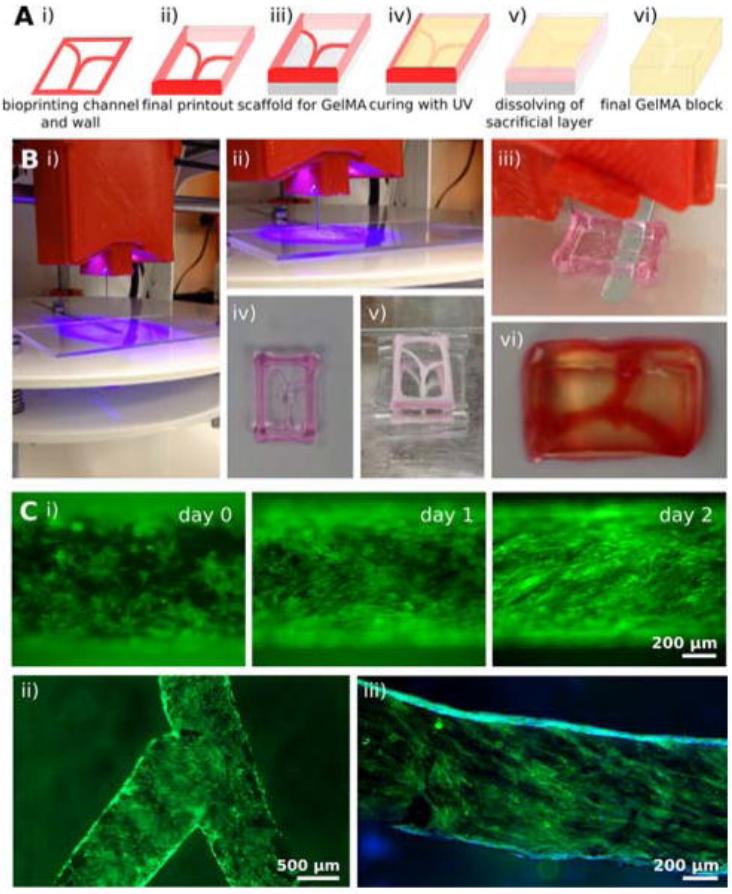

Figure 5: Sacrificial bioprinting of vascularized hydrogels. A) Schematic of the bioprinting process. B) Photographs showing the experimental depiction of the corresponding steps in (A). C) Endothelization of the hollow microchannels inside the GelMA construct. From [46].

The second strategy relies on the intrinsic properties of endothelial cells, which can spatially self-assemble to form vascular networks when seeded in 3D matrices. Kim *et al.* reported the use of ECs (seeded in a central channel of a PDMS-based microfluidic device) as vascular precursor cells, and stromal cells (seeded in the lateral channels) to support the ECs morphogenesis via secretion of pro-angiogenic growth factors and ECM proteins [47]. They used a fibrin matrix supplemented with collagen type I to recreate the physiological environment. After 5 days in culture, vascular networks spontaneously emerged in the central channel.

To better recapitulate vasculogenesis, Watanabe and Sudo (2020) reported the use of PDMS to fabricate a microfluidic chip in which the hydrogel's solution mainly composed by fibrin and collagen was injected through the inlet channel [48]. Then, the endothelial seeding was performed through the outer channels. Once ECs get attached to the scaffold, mesenchymal stem cells were injected through the channels promoting the formation of microvascular networks. Figure 6 shows a schematic of the process to obtain this VoC.

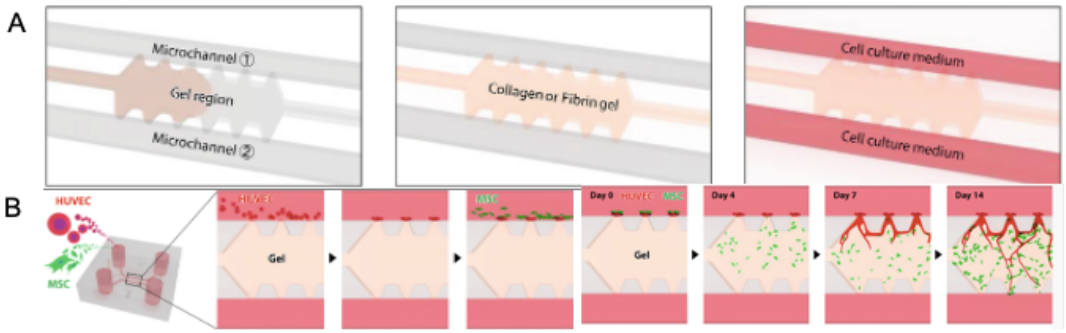

Figure 6: Schematic of the process to obtain a VoC to recapitulate vasculogenesis. A) Schematic of the injection of the hydrogel. B) Schematic on the cell seeding for both cell types. Adapted from [48].

3. Market analysis

OoC technology emerged approximately 10 years ago constituting a recent field in expansion. In fact, the global OoC marked reached a value of nearly $50.8 million in 2020, having increased at a compound annual growth rate (CAGR) of 50.5% since 2015 and it is expected to grow to $177.8 million in 2025 and to $350.8 million in 2030. This growth is attributed to the increasing demand for personalized medicine, the need to minimize financial losses, the substantial funding of public and private sources for OoC start-ups and research groups as well as the adoption of OoC technology by major pharmaceutical companies such as Roche and AstraZeneca [49].

One of the first papers detailing the use of organized cell cultures to study disease was published by Andre Kleber in 1991, in which the construction of a ventricular myocardium through the growth of cells *in vitro* was reported [50]. In 2004, Shuler *et al.* introduced the concept of mimicking the organ-level function of human physiology using cells inside a microfluidic chip with their work in which they captured the interaction between lung and liver on a silicon chip [51]. However, it was not until 2010 when the term OoC was proposed by Donald Ingber from Wyss Institute, who

reported the creation tissue-tissue interface of human-cultured epithelial and endothelial cells together, with an ECM device that modelled the alveolar-capillary interface of the human lung [50]. This same group, later in 2013, created Emulate, which was one of the first companies commercializing OoC devices. Currently, there are many other companies and start-ups developing OoC like Organovo, Alveolix, Nortis, TARA Biosystems or Synvivo, among others [52].

Nowadays, Emulate offers numerous platforms for modelling different organs such as brain, kidney, liver, lung and both colon-intestine and duodenum-intestine interfaces, which can be used to study multiple processes (e.g. inflammation and metastasis in cancer). Among other products, Emulate provides a VoC to recapitulate thrombosis. The chip is based on two microfluidic channels separated by a thin, porous membrane entirely covered with endothelial cells [53]. However, the thickness of the membrane does not match the thickness of the basement membrane of blood vessels. To overcome this limitation, hydrogels molded with a microchannel inside are being studied. In this context, MIMETAS stands out because they introduced hydrogel-liquid interfaces in their microfluidic chips to mimic ECM. Cells can be embedded in these hydrogels or grown on their surface to better resemble the tissue-tissue interface. Their system is versatile since allows the formation of biochemical and physical barriers to study of cell migration, (ii) 3D co-culture, perfusion, etc. Also, MIMETAS' OrganoPlate™ in a 384-well plate format offers a PDMS-free chip and one of the most compact and high-throughput OoC on the market. MIMETAS has also developed a VoC (OrganoReady ®Blood Vessel HUVEC) to investigate permeability, absorption and transport, toxicity and barrier integrity in blood vessels [54]. Each chip is composed by one in-gel culture channel and two perfusion channels, of which one perfused endothelial tubule. The gel is composed of collagen-I and injected through the culture channel.

The OoC market growth is highly related to the technological advances such as 3D bioprinting, which has made tremendous progress over the last years and has managed to print soft materials like hydrogels. Organovo (ONVO) is one of the first 3D bioprinting companies. They developed ExLive3DTM Liver model by directly depositing hepatocytes and nonparenchymal cells in 3D to form a liver module [55]. Currently, they are working with L'Oréal to 3D print human skin surrogates to test cosmetics. However, few companies have tried to implement 3D bioprinted hydrogels into microfluidic devices. Aspect Biosystems stands out as a developer of a microfluidic-based printing platform (Lab-On-a-Printer) that can dispense cells in an alginate-based hydrogel. With this technology, they developed the 3DBioRing™ Airway tissue by printing airway smooth muscle cells into a ring-like structure in a dish to model respiratory functions and diseases such as asthma that are characterized by airflow obstruction [56]. Despite these particular examples, the majority of big 3D printing companies, such as Regemat 3D, and Advanced Solution Life Science and Biobots, only provide for 3D bioprinters (technology) and not final commercial solutions [50]. This market was valued with 1.7 billion in 2021 and it is expected to grow at a compound annual growth rate (CAGR) of 15.8% from 2022 to 2023. This growth is attributed to the limited number of organ donors and an increasingly aging population with chronic diseases [57].

4. Concept engineering

OoCs are composed by a patterned material that contains the microchannels and the allocation for the cell culture, a substrate, connectors, tubes and a peristaltic micropump to control the flow in the channels as shown in Figure 7. The allocation will contain the 3D scaffold in which cells will be embedded and/or seeded on top. Both substrates are bonded by either chemical treatments, screws, or adhesives. Before the bonding, holes are made to the patterned material to insert the tubes and connectors that will be connected to the peristaltic micropump. In this section, detailed information is provided on the design considerations for the OoC model developed in this project. Firstly, the components of the microfluidic chip will be described, then information about the technology and material regarding the 3D scaffold to embed and seed cells will be provided. Finally, a description of the cells used and the methodology to assess viability of the embedded cells will be included.

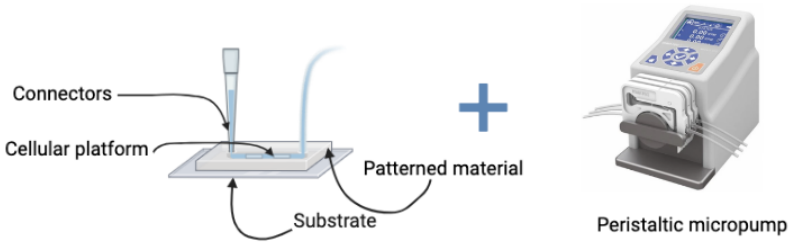

Figure 7: Schematic of the microfluidic set up to culture on an OoC. Elaborated in biorender.com.

4.1. Microfluidic chip

The design of a microfluidic chip for OoC's applications must ensure to meet several requirements including miniaturization, low-cost devices – referring to the technology, the materials, and the disposables –, low reagent consumption, fluid separation –achieved by ensuring independent channels –, and laminar flow [58]. For this purpose, in this section a review on the material, the geometry and the dimensions of the chip, the technology to develop them, the hydrogel printing process and the external casing is included.

4.1.1. Material

Choosing a suitable material is critical to obtain an efficient OoC since it affects the performance, monitoring, and the results of the experiments. In general, there are some requirements that must be considered when choosing the chip's material. These requirements are: optical transparency (to be able to be inspected using a microscope), gas permeability, non-toxicity to cells, low-cost, and the easy manufacturing technology [24].

In this project we aim to develop a PMMA-based chip composed by two PMMA sheets, one containing the pattern of the channels and the other one used for sealing the chip.

PMMA is a low-cost, low density, transparent, biocompatible material that can be easily manipulated to fabricate OoC. Because of its molecular organization, it is more resistant to pressure and temperature fluctuations than other materials like PDMS, which also ensure its chemical

stability and its suitability for biomedical/biochemical applications [24]. PMMA is one of the most common thermoplastic materials, so it becomes moldable at a certain elevated temperature and solidifies upon cooling. The temperature that must be reached to soften the polymer and make it pliable is known as glass transition temperature (Ts). In the case for PMMA the atactic PMMA's transition temperature is 398K (125ºC). However, since the commercial PMMA is often copolymerized with comonomers different that methyl metacrylate, the Ts can range from 360K to 430K [59]. This characteristic of thermoplastics makes them appropriate to be manipulated by hot embossing techniques or injection molding, for example.

4.1.2. Geometry and dimensions

According to the application of the OoC and the technology used to recapitulate the organ or tissue, there are several chip designs. However, a common approach to classify the different geometries in a chip is based on the number of channels they possess. According to this classification, OoCs can be single-channel chips, double channel chips – including parallel designs and sandwich designs -, and multichannel chips [24].

The most common design is the double-channel chip, in which they are separated by either a porous membrane or a hydrogel. The chip possesses two inlets and two outlets that control the entry and exit of the working fluid as well as the introduction of biological materials like basal laminal proteins, cells, and therapeutic drugs into the system. Although these chips are less challenging in terms of assembly and suitable to perform diffusion studies, for VoC applications they offer a less accurate microenvironment since the endothelial cells only contact the hydrogel through one side of the channel. For this reason, in this project a triple-channel chip was also considered to achieve an endothelial central channel completely surrounded by hydrogel, thus emulating a blood vessel. A schematic drawing of the geometry of both chips is provided in Figure 8. To ensure laminar flow, reservoirs are placed at the end of the channels. These reservoirs have a circular shape and determine the inlets and outlets of the system. Then, the fluid will fill this cavity before entering the channel, generating less turbulences in the flow.

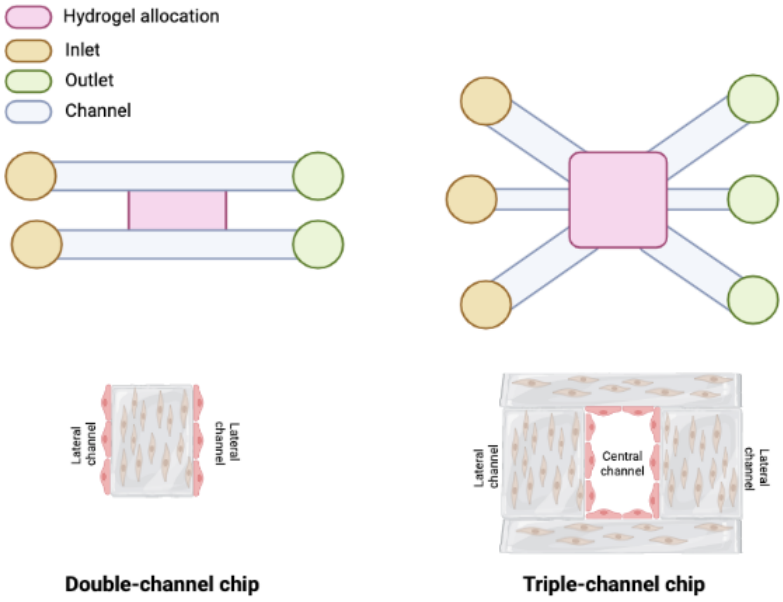

Figure 8: Schematic drawing of the channels geometry for the double-channel and triple-channel chip. Created in biorender.com.

The dimensions for the chips described in this project are depicted in Table 1.

Table 1: Dimensions for both geometries of the microfluidic chips.

	DOUBLE-CHANNEL CHIP	TRIPLE-CHANNEL CHIP
ALLOCATION	5 x 2 mm	5 x 3 mm
LATERAL CHANNELS	750 x 450 μm	750 x 600 μm
CENTRAL CHANNEL*	-	600 x 600 μm

Another important design consideration is how the hydrogel is placed in the chip. If the hydrogel is not released from the printing substrate, the patterned PMMA will require an allocation for it. This approach allows for less manipulation of the hydrogel, but additional leaking problems may appear. Whereas, if the hydrogel is released from the printing support with the help of a scalpel and tweezers, this additional allocation will no longer be needed. Figure 9 provides a schematic on these two possible chip geometries regarding the allocation for the printing support of the hydrogel.

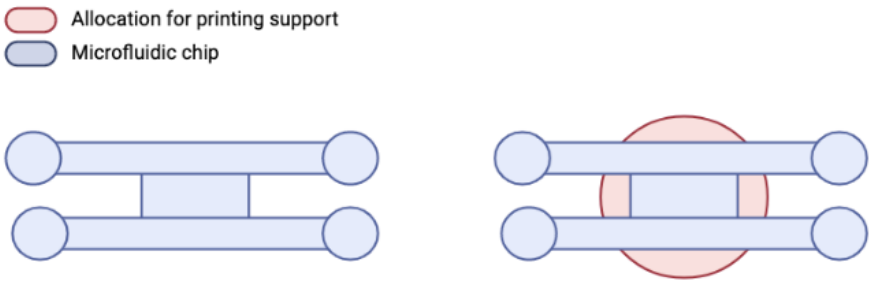

Figure 9: Schematic of the two possible chip geometries for the double-channel chip regarding the allocation of the printing support. Elaborated in biorender.com.

4.1.3. Fabrication technology

Microfabrication consists of miniaturizing devices. There are various techniques to add or remove materials and pattern a substrate with a desired geometry. The reported technologies to fabricate PMMA devices are injection molding, laser cutting and hot embossing [24], though in this project, only the last one was explored because of its speed and high reproducibility.

Hot embossing consists on transferring the pattern from a mold to a target material by applying heat and pressure. For that reason, the target material should be thermosensitive to soften once the Ts is reached and harden when the temperature is decreased. Meanwhile the mold must be made of heat conductive material. However, since the equipment to perform hot embossing is expensive and big, in this project we have adapted the equipment to reduce costs and keep the system in the lab. Qnubu press compact 2.0 manual 600kg was used since it allows for digital control of the temperature from 0ºC to 200ºC and can apply a pressure up to 600kg. We adapted the protocol (Figure 10). First, the patterned mold and the PMMA sheet are aligned and placed between the heating plates. The lever is lowered until both heating plates are in contact with the materials. This sandwich is then heated to 80ºC, maintained this temperature for 200 s, and the temperature was increased to 130ºC. Once this temperature was reached, pressure was applied

for 5-10 min by lowering the lever applying force. After, the system was cooled down to 80ºC maintaining the pressure. Finally, pressure is released, and the system is turned off to cool down the plates and remove the pieces.

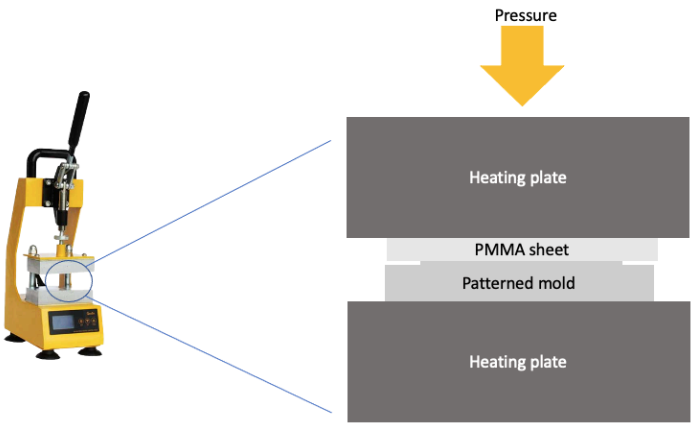

Figure 10: Adapted hot embossing technology.

The technique was explored using resin and aluminum molds. Resin molds were 3D printed with Phrozen XL Shuffle stereolithography (SLA)-based printer using Gray ABS like resin (Phrozen ABS like Resin Matte Grey 0.5 mm). Briefly, the resin is photocured layer-by-layer according to a CAD design using a 405 nm LED-based LCD display. Once the printing is finished, a post-processing step is required to remove the remaining resin and obtain the final objects. The printed pieces are removed from the building plate with a scalpel and then, firstly, they are immersed into a dissolvent (Phrozen Resin Wash) for 2 minutes, secondly, plunged in Resin Away (MonoCure 3D ResinAway) for 5 minutes and thirdly, they are put in water to remove the remaining dissolvents. Finally, they are dried with a nitrogen gun and put in an ultraviolet (UV) lamp for 5 minutes to harden the pieces. Therefore, resin molds can be easily fabricated in the laboratory and allowed for the design validation. However, these resin molds only resisted one or two hot embossing processes before breaking. Thus, one the design was validated, the final mold prototypes were fabricated in aluminum in Fundació CIM (Universitat Politècnica de Catalunya). Aluminum is an excellent thermal conductive material and allows for better transfers of the pattern and multiple uses.

4.1.4. Hydrogel fabrication

4.1.4.1. Bioink preparation

Hydrogels were used as scaffolds to support the growth of the stromal cells inside as well as the endothelial cells on the surface. The bioink, optimized previously was composed of 5% (w/v) of GelMA, 1.25% (w/v) of PEGDA (Sigma-Aldrich), 0.2 % (w/v) of LAP (TCI Chemicals) and 0.025% (w/v) of tartrazine (Sigma-Aldrich) as a photoabsorber. The components were dissolved in Hank's Balanced Salt Solution (HBSS) (Gibco) supplemented with 1% (v/v) Pen/Strep at 65ºC for 2h to obtain the final bioink.

4.1.4.2. 3D bioprinting of the hydrogel

Hydrogels were fabricated using digital light processing (DLP)-SLA bioprinting. The printing set-up was obtained by modifying a commercially available Solus 3D printing equipment (Junction3D) together with a DLP projector-based SLA printer. The system consists of an aluminum vat with a transparent window, an aluminum building plate, and a beam projector. The vat is characterized by its small dimensions adapted to the size of hydrogels and can be heated to 37ºC, which is relevant to preserve the polymer solution in a liquid form and allow the use of cell-laden hydrogels. Fluorinated ethylene propylene (FEP) film (Junction3D) of 150 µm thickness was used to create a flexible transparent window in the bottom of the vat to allow the pattern transfer to the prepolymer solution and the permeability of oxygen to tune the polymerization reaction. The building plate is also adapted to the size of the hydrogel, and it is attached to a building platform which has a z-actuator where the printing surface (PET or coverglass) is attached, and the hydrogel will be printed. Finally, the light is projected through a High-Definition 1080p resolution projector (Vivitek) coupled to a short pass heat protection filter (Schott) that cuts off infrared wavelengths to avoid cell damage and allows light projection to the visible range. A schematic of the modified Solus 3D printing set-up (Figure 11A) and of the printing process (Figure 11B) is included below.

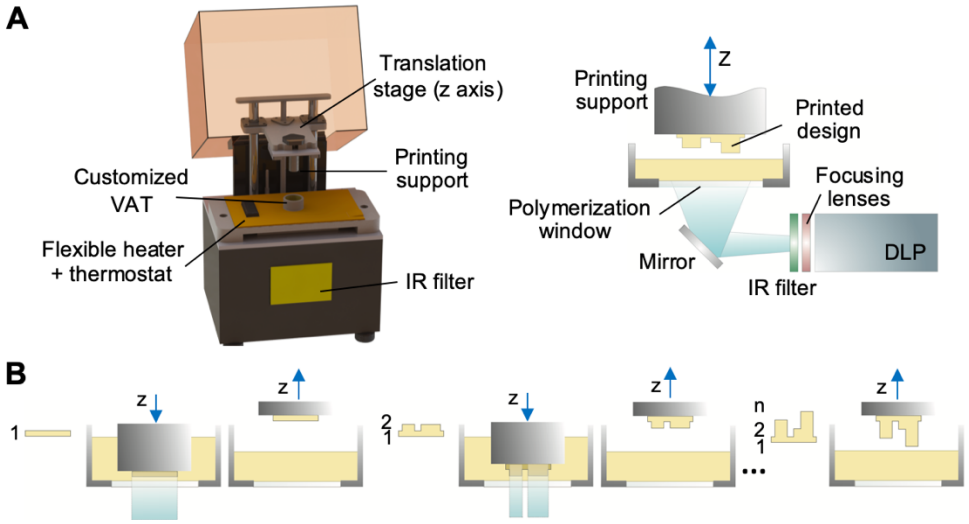

Figure 11: Schematic of the modified Printing equipment (A) and of how the hydrogel is printed with SLA Printing (B). From [33].

The printing process included several steps. First, a 3D CAD design with the desired structure is created in the software program FreeCAD. Two different designs were developed depending on the final chip design (Figure 12). On the one hand, a *rectangular-shaped* hydrogel was designed to fit in the double-channel chip. Several dimensions were considered so that, after hydrogel swelling, the hydrogel could fit in the allocation (5x2 cm). On the other hand, a *U-shaped* hydrogel was designed for the triple-channel device. Again, different dimensions were explored.

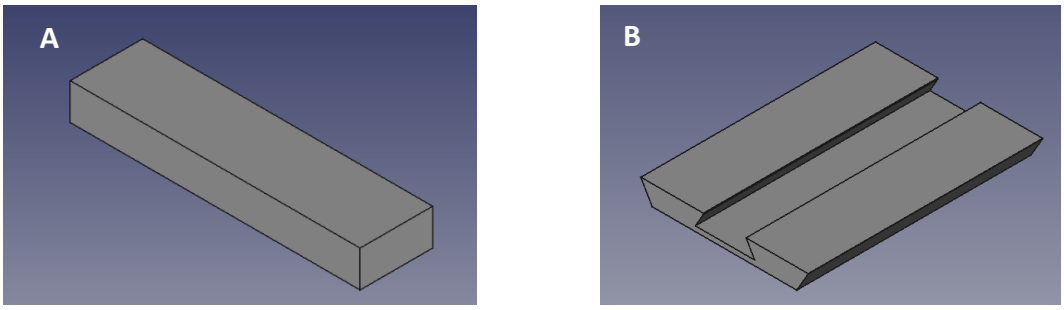

Figure 12: Hydrogel FreeCAD designs. A: RH for double-channel chip. B: UH for triple-channel chip.

The desired design is uploaded to the printer and the proper printing parameters, regarding build resolution and layer thickness and exposure, are chosen based on previous optimizations (Table 2).

Table 2: Printing parameters with solution

Layer thickness	20 μm
Layer exposure time	15 s
Initial layer exposure time	30 s
Number of initial layers	2
Exposure buffer time	1 s

Then, the polymer solution is introduced to the vat, the building plate is lowered until it is submerged into the mixture and the light projection begins. This light projection is performed according to a pattern depending on the uploaded design and the printing parameters. This pattern triggers the polymerization of a thin layer. To continue the printing and polymerize the following layer, the building plate moves upwards in the z-direction and the same procedure is performed. Therefore, the polymerization of the solution is performed layer-by-layer until obtaining the desired 3D structure. After printing, hydrogels were rinsed in warm PBS to remove the remaining solution, removed from the building plate and placed on a 24 well-plate (ThermoFisher Nunclon™ Delta Surface) is PBS or cell media (when cells were embedded inside) to perform swelling before being assembled in the microfluidic chip.

4.1.5. External casing

A functional OoC should be properly bonded to prevent leakage and to ensure independent flow channels. For that reason, bonding must be performed between the material containing the microchannels (in our case PMMA) and a substrate, that can be either solid, flexible or made of several materials. This sealing is highly dependent on the physical and chemical nature of the used materials [24].

Microfluidic bonding techniques can be classified as either direct or indirect. On the one hand, indirect bonding involves the use of adhesive layer to seal two substrate and encapsulate microchannels fabricated in one of the substrates. On the other hand, direct bonding does not use

any additional material to bind the surfaces and involves thermal fusion bonding, surface modifications and solvent bonding, among others [60].

In this project we have considered two bonding methodologies. However, before sealing the chips, the previously printed hydrogels must be released from the building plate and introduced inside their respective allocations. Depending on the sealing approach, the methodology to place the hydrogel inside was slightly different (see Figure 13).

In the first approach, also referred to as adhesive approach, pressure-sensitive adhesive (PSA) was used to seal the chip with the help of a scrapper. In this case, the only PMMA substrate used was the one with the pattern (with the allocations to accommodate the hydrogel, and the Polyethylene Terephthalate (PET) coverslip used as printing substrate, and the channels). With this methodology, the hydrogel printed on top of the PET substrate was placed in the allocation upside down, so that the hydrogel is in contact with PMMA in one side and PET in the other side.

In the second approach, also referred to as screw's approach, two PMMA substrates were bonded with screws. Moreover, a PDMS layer and a PET layer were included: PDMS is used to distribute the force applied by the screws more homogeneously because of the material's elastic properties, and the PET substrate was used to provide cells with the more similar substrate stiffness as possible to avoid their accumulation in one side of the hydrogel. In this case, the hydrogel was released from the coverglass and placed inside the allocation.

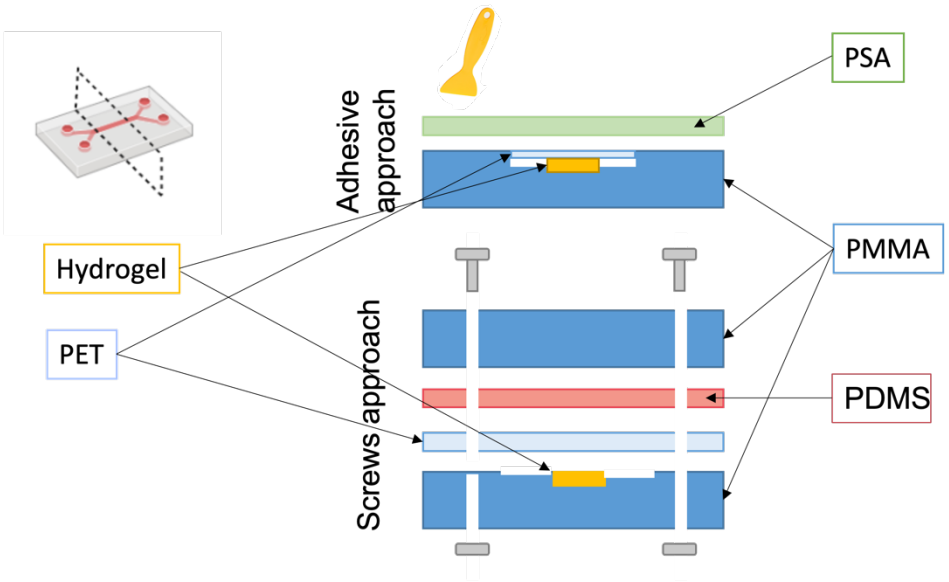

Figure 13: Cross-section view of the two bonding techniques using adhesives or screws.

Another relevant aspect in this second bonding approach is how screws are distributed to avoid leakage. Several sketches were designed and tested to select the final pattern. As previously mentioned, the reservoirs are the spaces in which the liquid will enter the device, and therefore, to avoid leakages one must ensure the complete sealing around them and the channels. Figure 14 shows the different distributions studied for each chip. In chips with two channels, design A was

the simplest one because it has the least possible number of screws located around the hydrogel to keep it wet, whereas design B was performed to avoid leakage before the entrance of the liquid in the channel. According to the results obtained through the validation of the double-channel chip, the distribution for the screws on the triple-channel chip was performed (design C and D).

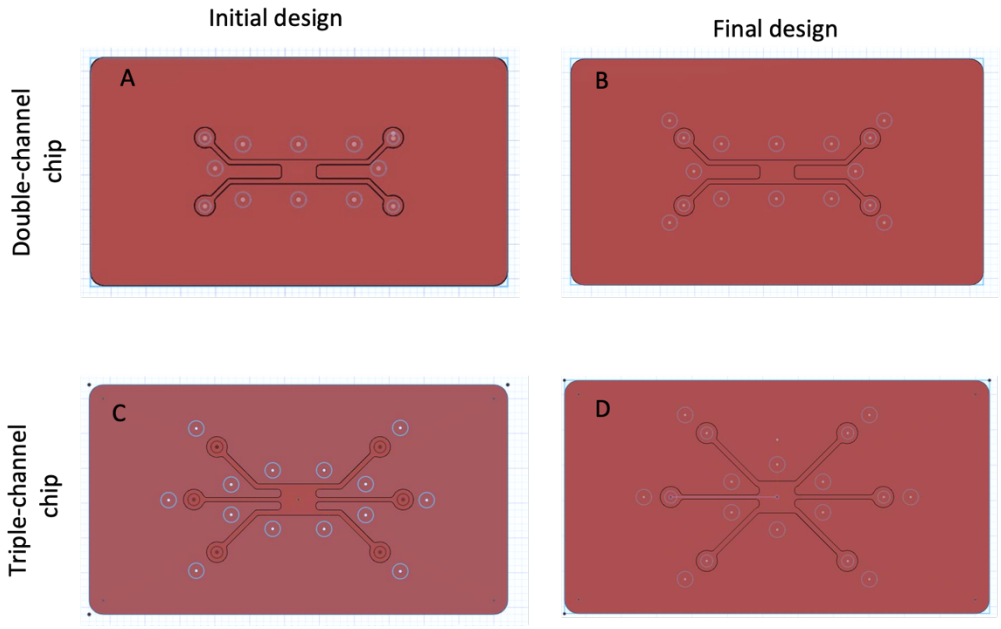

Figure 14: Top view of the screws's distribution in the double-channel and triple-channel chip.

4.2. Microfluidic set-up

4.2.1. Flow control

Controlling the flow rate is important to obtain accurate results since it affects the shear stress, polarity, concentration gradients of oxygen and nutrients, among other parameters. This control is achieved with pressure-driven systems like peristaltic micropumps and syringe pumps, which are the most common devices to use in practice. Due to the channels' dimensions, the flow is laminar (low Reynolds Values), and the values depend on the application of the OoC [24]. In this project 5 ml/min flow was applied to the tubes.

4.2.2. Tubes and connectors

To connect the microfluidic chip to the pump, two different tubes were used. First, PTFE tubes (internal diameter (ID) of 0.8 mm and external diameter (OD) 1.58 mm) were placed into the corresponding 1.5 mm holes of the PMMA chip applying pressure. These PTFE tubes were connected to flexible silicon tubes of 0.76 mm (ID) and 1.65 (OD), which in turn, were connected to the pump using Luer connectors. Figure 15 shows the complete microfluidic set-up to maintain the cells in culture inside the chips.

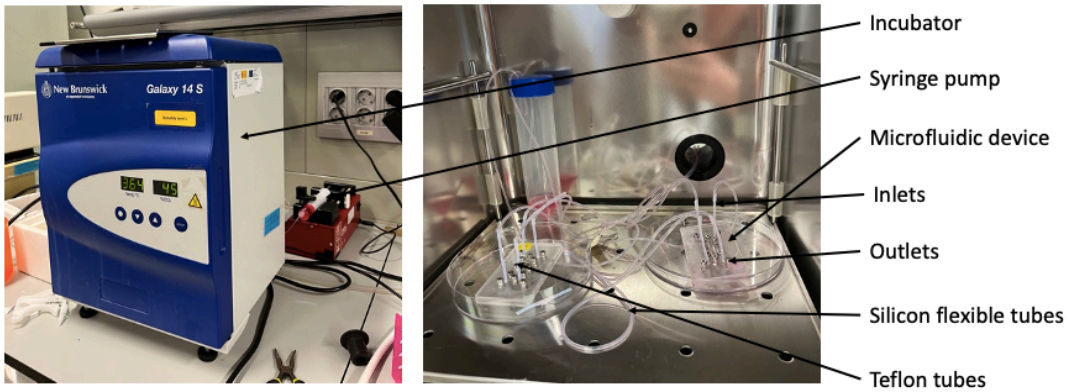

Figure 15: Microfluidic set-up.

4.3. Cellular component

To recapitulate a blood vessel, cells must be introduced in the microfluidic device. Since blood vessels are supported by an ECM that contains fibroblasts, these cells are encapsulated in the printed hydrogels. In this project, two cell types were used for encapsulation: NIH-3T3 and CCD18-Co. Both cell types are adherent cells that are characterized by having an elongated shape. NIH-3T3 is a mouse embryonic fibroblast cell line cultured in flasks with Dulbecco's Modified Eagle's Medium (DMEM Medium) (Gibco) supplemented with 10% (v/v) of Fetal Bovine Serum (FBS) (Gibco) and 1% of (v/v) Penicillin/Streptomycin (Pen/Strep) (Sigma-Aldrich). These cells were used because of their high growth rate. CCD18-Co are colon-derived myofibroblasts from a healthy woman. These cells are cultured in high glucose DMEM phenol red supplemented with 10% (v/v) FBS, 1% (v/v) Pen/Strep, and 1% (v/v) of non-essential amino acids (NEAA). In this case, they were used because it is a human-derived cell line.

For cell encapsulation, NIH-3T3 or CCD-18Co were trypsinized and counted to have a concentration of $7.5x10^6$ cells/mL. In the trypsinization process, cell medium is removed, and cells are washed in warm PBS. Then, cells were incubated in Trypsin-EDTA (Thermo Fisher) solution for 5 minutes or until cells were detached from the surface. The trypsinization reaction was inhibited by adding supplemented DMEM to the flask. Finally, the desired volume of cell suspension was extracted and centrifuged at 1200 rpm for 5 minutes. After centrifugation, the supernatant is carefully removed and directly resuspended in the polymer solution, to obtain the cell-containing bioink.

4.3.1. Cell viability assay

After several days of culturing the cells in the chip, the chip was disassembled, and the hydrogel was washed three times with warm PBS. Meanwhile, a mixture of 4 mM ethidium homodimer-1 (EthD-1) which is used to stain the nuclei of dead cells in red, 2 mM calcein AM which stains living cells in green and 20 mg/mL Hoechst which stains the nuclei of all cells, was prepared in warm PBS. Hydrogels were incubated with the solution for 20 min and then, washed thoroughly with warm PBS. The samples were analyzed with the confocal microscope (Zeiss LSM 800 Confocal Laser Scanner Micro) and quantified manually in ImageJ.

5. Detailed engineering

5.1. Microfluidic chip

5.1.1. Fabrication technology

The adapted hot embossing technique allows for the manipulation of the PMMA to get patterned according to the motifs of mold. We compared the performance of two different molds: resin-based molds obtained through 3D printing and aluminum molds fabricated in an external supplier. This characterization was performed comparing the average depths of the cavities for the hydrogel from different patterned PMMA sheets and different designs. Measurements were done with a caliper.

Figure 16 shows the performance of the technology using resin molds, in which A, B and C are different explored preliminary designs. Since the printer calculates the number of layers required depending on the CAD dimensions, the type of resin used and the layer thickness specified, the printed molds did not have the same dimensions than the CAD design. Moreover, as shown in the figure, 25% of resolution was lost during transferring step of the pattern in the PMMA sheet, which was attributed to the low thermal conductivity of the resin. Despite these inaccuracies, the resin molds were used to optimize the different designs of the chip before fabricating the final prototype in aluminum.

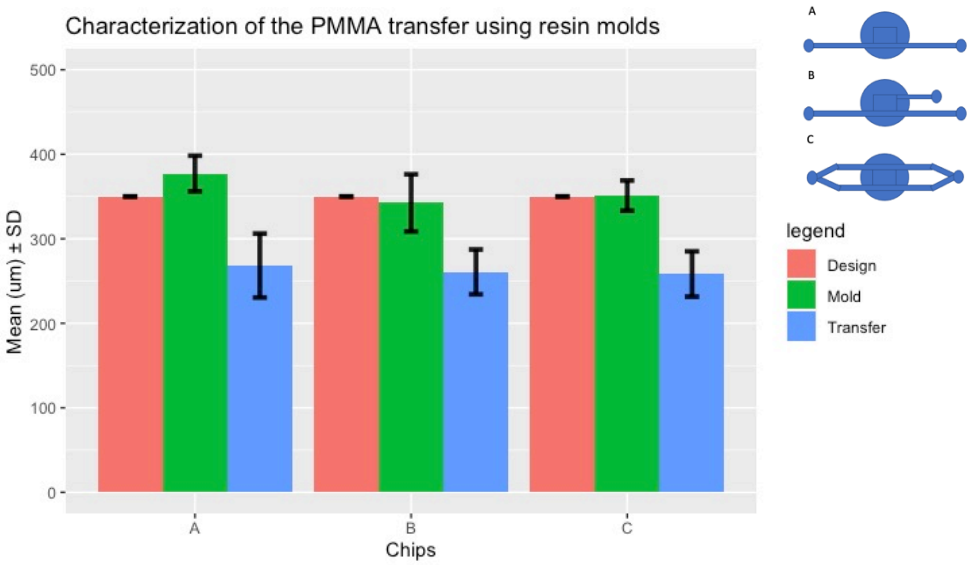

Figure 16: Characterization of the adapted hot embossing technique using resin molds obtained through 3D printing.

Thus, after the design optimization and to increase the resolution of the transfer, aluminum molds were used despite their higher cost with respect to resin molds and the externalization of the fabrication. As depicted in Figure 17, the achieved dimensions in the PMMA corresponded to the dimensions in the design, achieving high resolution and high reproducibility in the fabrication of patterned PMMA by hot embossing.

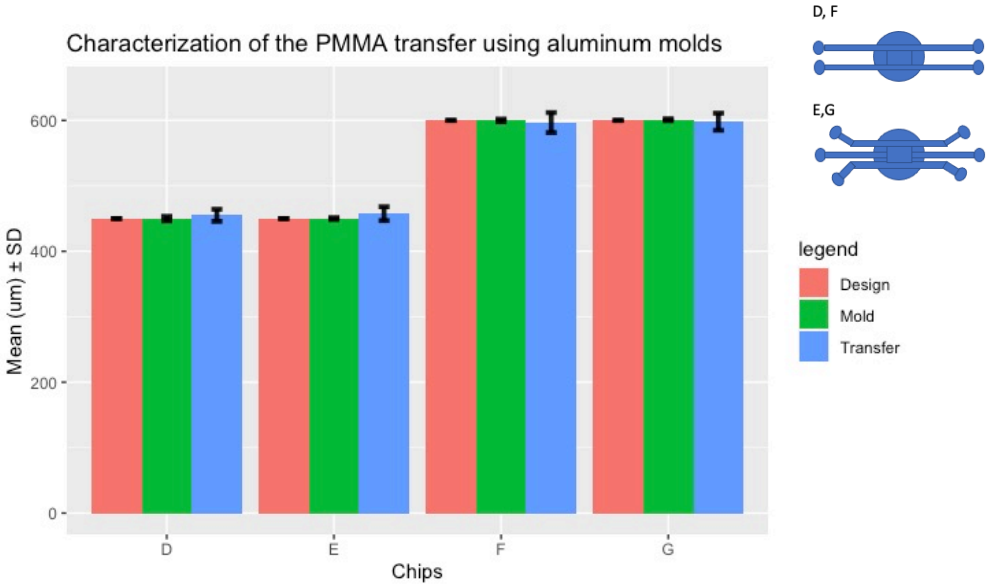

Figure 17: Characterization of the adapted hot embossing technique using aluminum molds.

Therefore, this equipment allows for an easy manipulation of thermosensitive materials like PMMA, while reducing costs. Moreover, its low dimensions allow the equipment to be settled in the laboratory and easy to access. Finally, it has been demonstrated that aluminum molds increase the resolution of transfers and increase the reproducibility of the fabricated chips. However, resin molds were used to test the performance of the several designs in terms of geometry and bonding methods.

5.1.2. External casing

Two different methodologies were studied regarding the external casing design: the adhesive approach and the screws approach.

Using the adhesive, the hydrogel bioprinted on top of the PET substrate was sealed to the PMMA transferred sheet using PSA. In this approach, Teflon tubes were introduced to the chip and fixed in the hole with Araldite EPOXI glue. This sealing technique was easy, fast, and required less manipulation of the hydrogel containing cells. Moreover, this approach allowed the inspection of the cells cultured in the chip with an optical microscope. Nevertheless, in this approach, the hydrogel must be printed at the center of the PET substrate. During the printing process, the right coordinates must be selected and in every experiment. However, as shown in Figure 18, channels were not independent and the fluid mixes along the circuit because of the leakage between the PET substrate and the allocation.

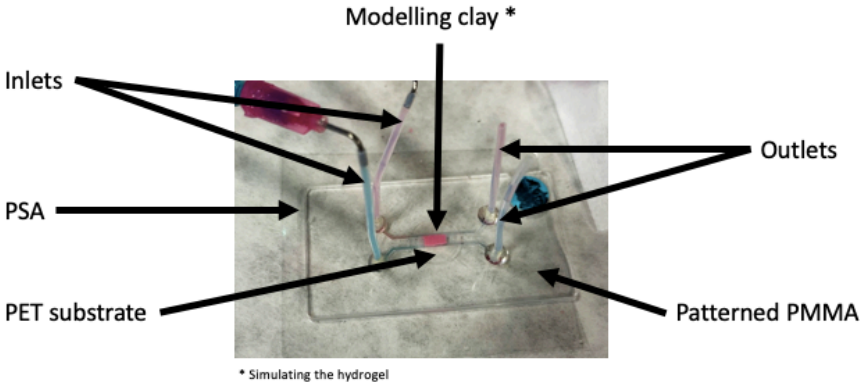

Figure 18: Microfluidic chip sealed with the adhesive approach.

Therefore, a second approach was explored. This approach was based on the use of screws to apply pressure and avoid leakage. In this case, the hydrogel was released from the printing support (either PET or coverglass) and placed in the cavity of the patterned PMMA. This step, also referred to as manipulation step, was very critical, due to the hydrogel tendency to fold and to attach to surfaces. The sealing was achieved by adding a layer of PET film, a PDMS sheet and a second PMMA sheet to the patterned PMMA with the hydrogel. This approach generated a "sandwich" that was bonded with screws. Several designs were studied to properly distribute the screws to avoid leakage and maintain channels independency (Figure 14). For the double-channel chip, design A was discarded because the fluid leaked even before arriving to the channels, in between the layers of PMMA. However, adding screws around the reservoirs (design B) solved the issue (Figure 19, left panel). For the triple-channel chip, design C was also ruled out because the exerted pressure was too high that channels were clogged, preventing the fluid from going through the device. Finally, the performance of the device with design D showed good results (Figure 19, right panel).

Even though with this second approach, the independency of the channels was achieved, the manipulation of the hydrogel was high, leading to a low yield of successful chips (several hydrogels must be discarded if they fold on themselves or break during the manipulation step). Nonetheless, this option is the preferred approach regarding the sealing methodology to obtain the final design.

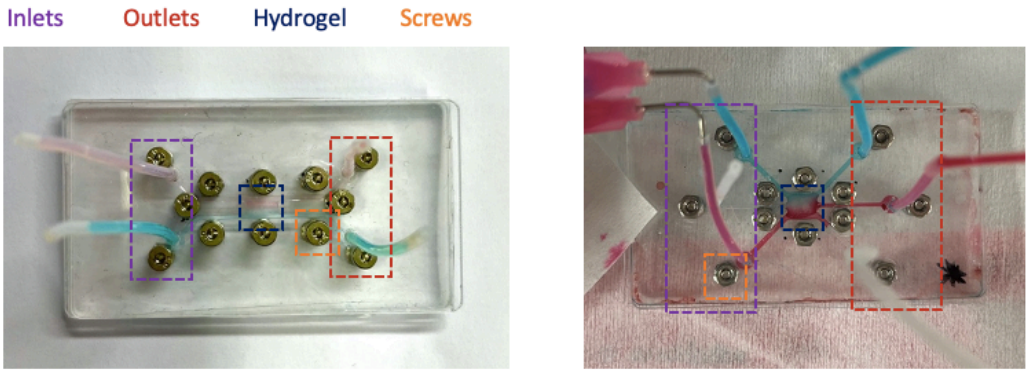

Figure 19: From left to right: double-channel and triple-channel microfluidic chips sealed with the screws approach according to design B and design D, respectively.

5.2. Hydrogel design and optimization

5.2.1. Double-channel chip

Hydrogels swell when being in contact with water or other liquid substances, resulting in a change in the dimensions compared to the CAD design. Specifically, hydrogels bioprinted with our bioink achieved its maximum swelling stage after 4 hours of being in a 24 well-plate in PBS [61]. Due to this change in dimensions, it is important to adjust the initial dimensions of the designs in order to fit in the allocation after swelling. In this context, several hydrogel's dimensions were studied (Table 3).

Table 3: Hydrogel dimensions studied to fit in the allocation for the double-channel chip

	ALLOCATION DIMENSIONS	HYDROGEL RANGES
LENGTH	5 mm	4.5 – 5 mm
WIDTH	2 mm	1 – 2 mm
THICKNESS	450 μm	300 – 450 μm

Finally, the selected dimensions for the CAD design of the rectangular-shaped hydrogel were 4.8 x 1.5 mm (see Figure 20). The thickness of the printed hydrogel depended on the sealing technique used. For instance, when bonding was achieved with PSA, the hydrogel thickness was 400 μm. Whereas in the screws approach, hydrogels measured 300 μm.

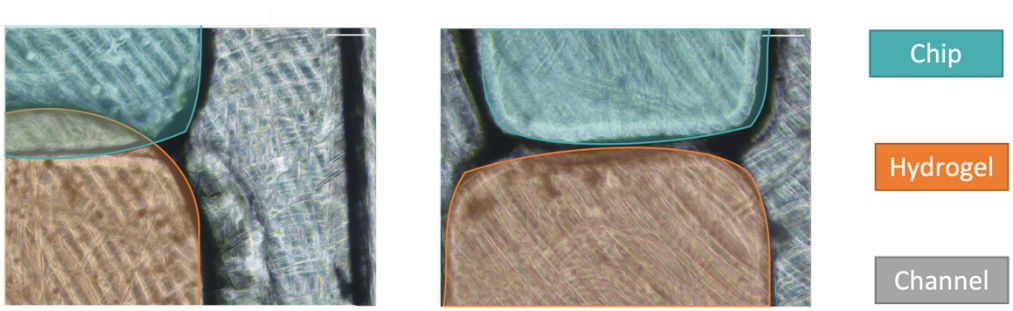

Figure 20: Photographs showing the adjustment on the length of the hydrogel from an initial approach (left panel) when the hydrogel measures 5 mm in length to the final approach (right panel) in which it measures 4.8 mm. Scale bar: 100 μm.

5.2.2. Triple-channel chip

The same study was performed for the U-shaped hydrogel to fit in the triple-channel chip design. In this case, besides adjusting the length, width and thickness, the channel dimensions were also adjusted.

In this chip, the allocation was bigger (5 x 3 cm) and had the same size than the hydrogel design in terms of length and width. However, before reaching this conclusion, several trials were done to adjust these parameters (Figure 21).

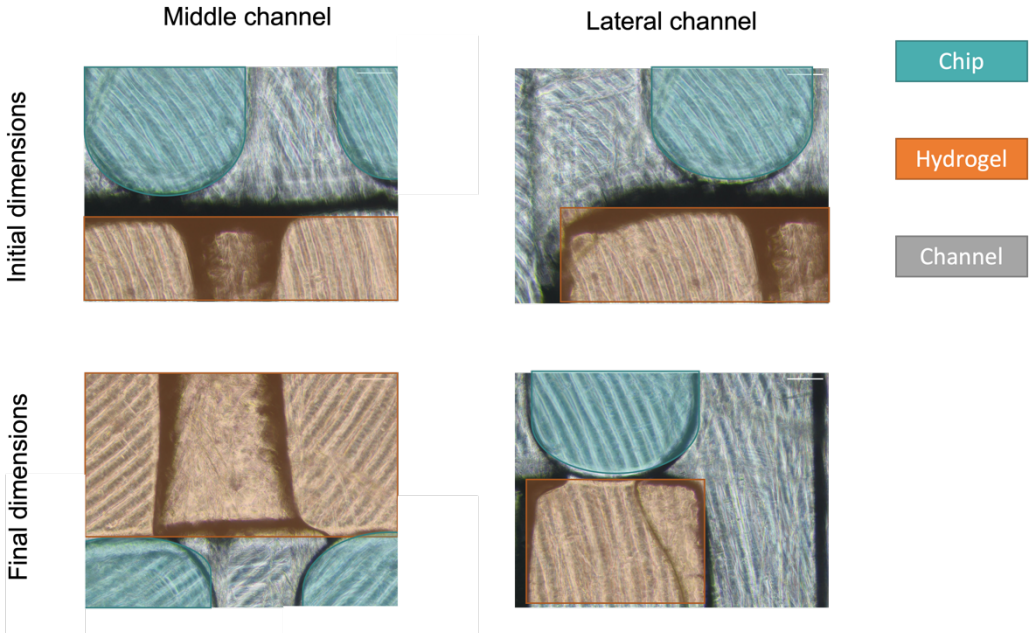

Figure 21: Comparison of the initial and final U-shaped designs in terms of length and width. Scale bar: 100 µm.

In addition, in this design, the U-shape dimensions had to be adjusted too. As shown in Figure 22D, the final design of the hydrogel had sharper edges than in the initial design, which was achieved by applying a correction in the design (see Figure 22C). Moreover, the channel width was reduced.

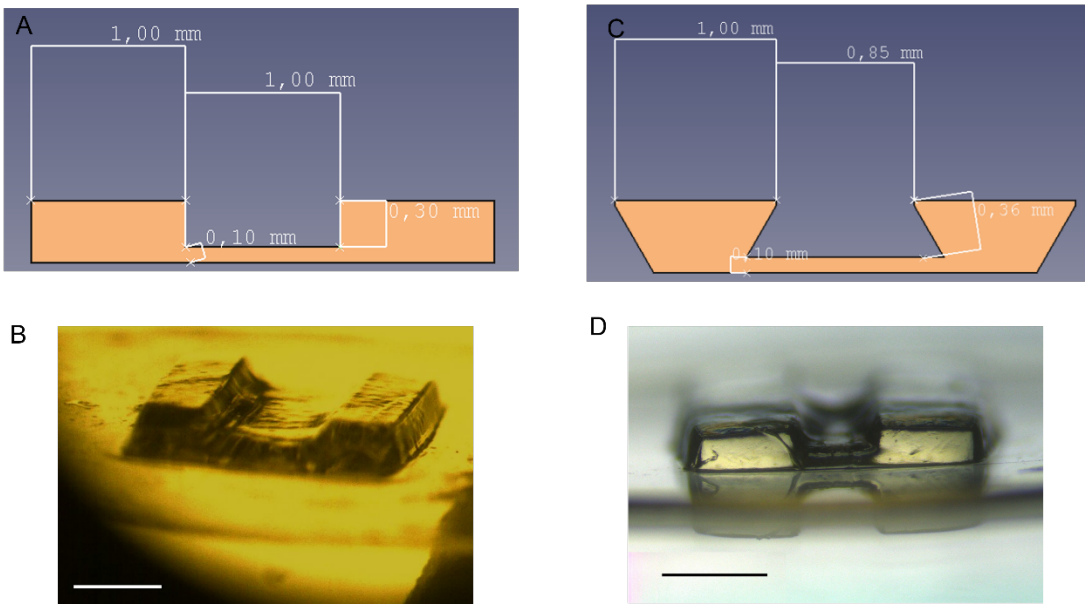

Figure 22: Comparison of the initial and final U-shaped designs. A) Example of a printed U-shaped hydrogel with the first design. B) CAD design and dimensions of the first approach. C) Example of a printed U-shaped hydrogel with the final design. D) CAD design and dimensions of the final approach. Scale bar: 1mm

5.3. Cellular component

In order to assess the viability of the cells encapsulated within the hydrogel, cell-laden hydrogels were assembled in the double-channel microfluidic chip. Therefore, hydrogels were rectangular in

shape with previously optimized dimensions to fit in the allocation of the chip and contained fibroblasts (NIH-3T3) and myofibroblasts (CCD18-co) embedded. The hydrogels were assembled in the chip following the two bonding approaches previously detailed: the adhesive approach or the screw approach. Medium was then introduced with an external pump at 5ul/min rate. Several experiments were performed to determine the viability of cells inside the chip for each bonding technique.

On the one hand, NIH-3T3 cells were embedded in two hydrogels and incorporated in two double-channel microfluidic chips sealed with the adhesive approach. Two time points were selected to perform the Live/Dead™ assay: after 1 day or 7 days under flow with media. However, at day 6, the microfluidic chip seemed contaminated, and the chip was disassembled. Inspecting the hydrogel in the optical microscope, we observed that cells were elongated at the laterals and corners of the chip (Figure 23) and there were no signs of contamination. Thus, the sample was transferred to a 24 well-plate with fresh media and placed in the incubator until performing the Live/dead assay the following day.

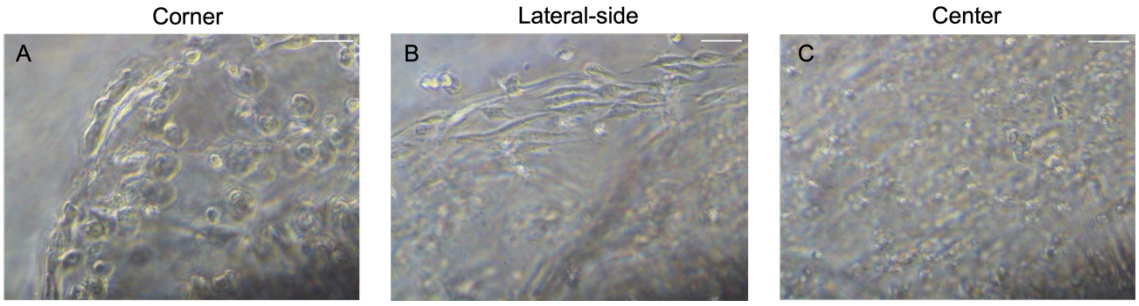

Figure 23: Hydrogels with embedded NIH-3T3 cells. A) Hydrogel corner, B) Lateral side facing the channel and C) center of the hydrogel. Scale bar 100 µm.

Then, a Live/Dead™ assay was performed to evaluate the cell viability (Figure X). Cell-laden hydrogels cultured in static conditions (in 24-well plates) were used as controls. Calculation was performed considering that all nuclei were stained in blue with Hoechst, living cells were depicted in green and dead cells in red. For quantification, cells with double staining green and red were considered to be dead. Photos were taken at different locations of the hydrogel (lateral and center) (Figure 24).

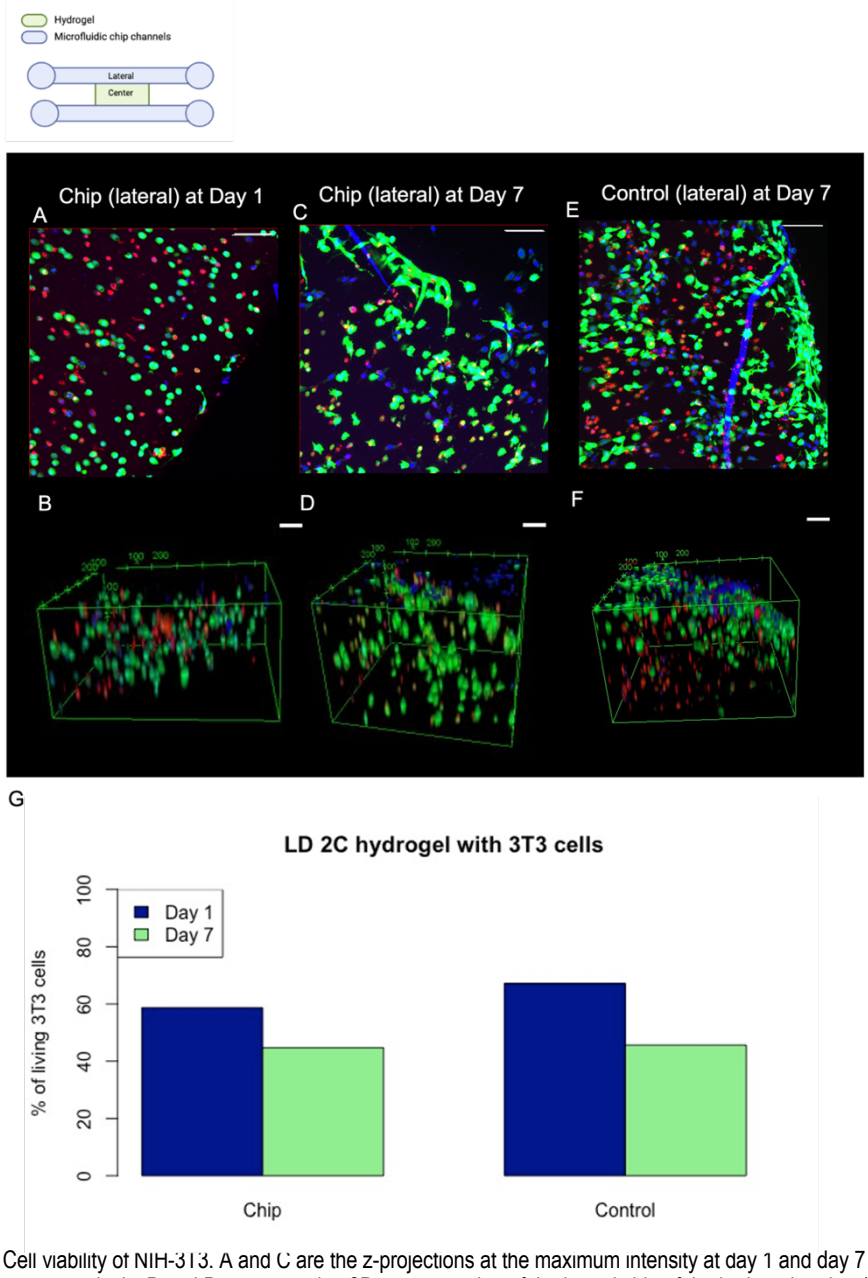

Figure 24: Cell viability of NIH-3T3. A and C are the z-projections at the maximum intensity at day 1 and day 7 after culture in the chips, respectively. B and D correspond to 3D reconstruction of the lateral side of the hydrogel at day 1 and day 7 respectively. E and F are the z-projections and 3D reconstruction of the lateral side of the control hydrogel at day 7, respectively. G shows % of living NIH-3T3 cells at day 1 and day 7 of culture inside the chip and in well-plates (control).

Cell viability was found to be 60% at day 1 when cells were perfused with medium and decreased to around 50% after 7 days under flow conditions. These values were not as high as expected. However, taking into account that the chip was contaminated, some channels were clogged with air bubbles, and the cell viability in controls was not very high either, this result is acceptable.

In order to test the cell survival in the chip using a different cell line, a second experiment was conducted with human CCD18-co myofibroblasts encapsulated in two hydrogels with the same characteristics as in the previous experiment. They were assembled in two double-channel microfluidic devices, which were sealed with adhesive and connected in series. However, since the channels were not independent the second chip, which had its inlets connected to the outlets of the first chip, did not received the proper media flow. In this experiment, chips were disassembled

after 1 day under flow and the viability was analyzed with the live/dead assay (Figure 25). Results show high cell viability rates in the first chip and in the static control. However, the viability of the second chip was highly compromised due to the lack of flow previously mentioned. These results confirm that the PMMA-based chips were able to sustain the viability of cells encapsulated inside the hydrogel, but the channels were not independent and there were some leakage problems that led us to change the bonding strategy.

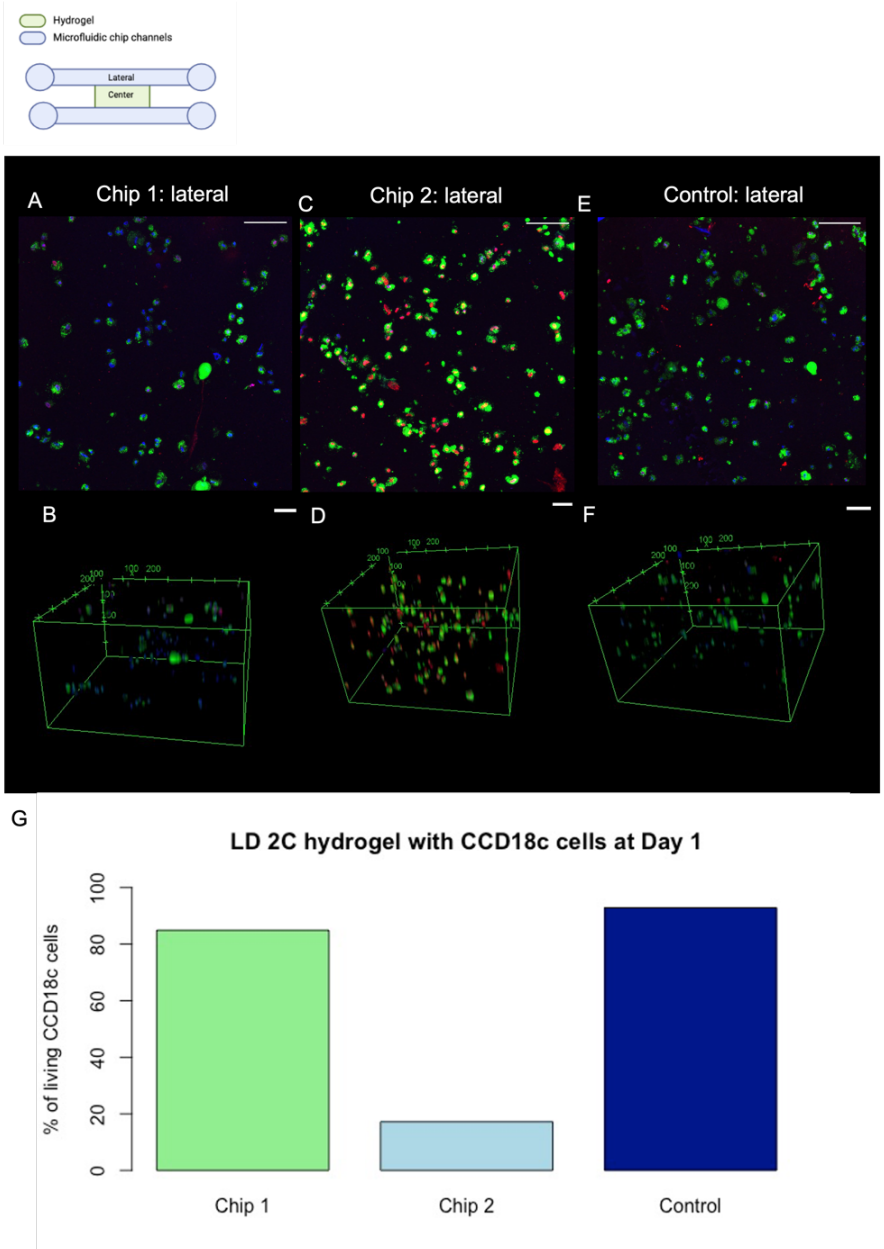

Figure 25: Cell viability of CCD18-co. A and C are the z-projections at the maximum intensity at day 1 after culture in the two different chips. B and D correspond to 3D reconstruction of the lateral side of the hydrogel at day 1. E and F are the z-projections and 3D reconstruction of the lateral side of the control hydrogel at day 1, respectively. G shows % of living CCD18-co cells at day 1 of culture inside the chips and in well-plates (control).

Finally, a last set of experiments was conducted to assess cell viability when the technique used for bonding was based in screws (Figure 13). As mentioned before, this technique implied high manipulation of the cell-laden hydrogel. Again, double-channel chips were used with rectangular hydrogels encapsulating NIH-3T3 cells. However, although the leaking problems were solved and

the flow channels were independent, we faced several contaminations of the experiments that had to be discarded. To avoid further contaminations, all the components for the chips as well as the microfluidic set-up were left in 70% (v/v) bleach for 2 days, and in 70% (v/v) ethanol for 2 more days. Then, they were disinfected with UV radiation in the cell culture tiny hood for 2 hours. Lastly, double-channel chips were assembled and kept under flow for 4 days. Then, they were disassembled and cell viability was assessed in one of the chips (Figure 26).

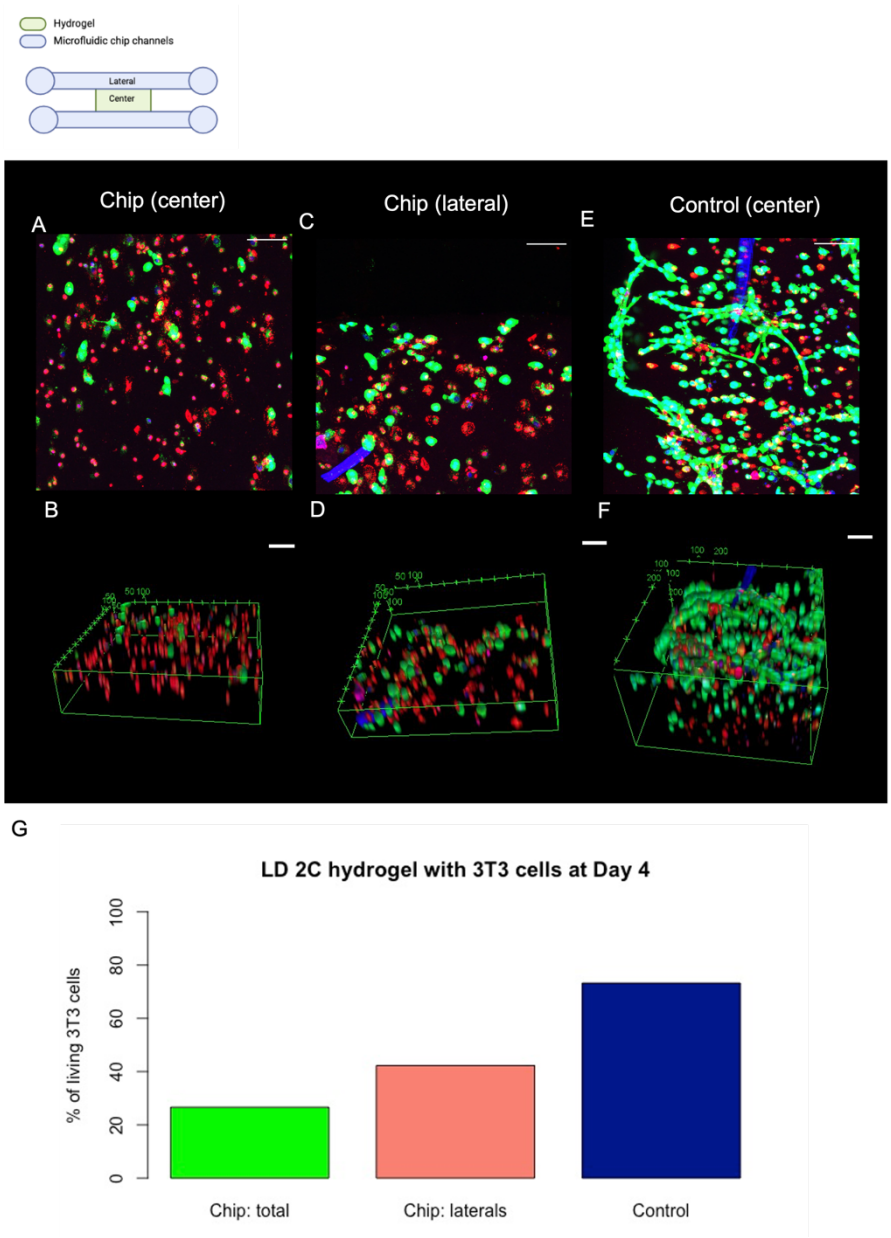

Figure 26: Cell viability of NIH-3T3. A and C are the z-projections at the maximum intensity at the center and laterals after 4 days in culture in the chip, respectively. B and D correspond to the 3D reconstruction of the center and lateral of the hydrogel, respectively. E and F are the z-projections and 3D reconstruction of the center of the control hydrogel at day 4, respectively. G shows % of living NIH-3T3 cells at day 4 of culture inside the chip and in well-plates (control). Scale bar 100 µm.

We observed that the cell viability rates of the chip were very low, especially in the center of the chip. A possible hypothesis would be that the perfusion of the medium going through the channel could not reach all the embedded cells since results show that the cells facing the channel had higher viability than the central part. However, if this was the cause of the low cell viability, we would

have had similar results in the previous experiments. Therefore, this result might be attributed to cell damage during the manipulation of the hydrogel during chip assembly, which includes its releasing from the coverglass printing support and the introduction of the hydrogel to the cavity.

Nonetheless, further experiments should be carried out to confirm this hypothesis. If the hypothesis is verified, it would be necessary to redesign the set-up to improve cell viability inside the chip, while avoiding leakage and communication between channels.

6. Execution schedule

6.1. Work Breakdown Structure

Figure 27 depicts the Work Breakdown Structure of the project.

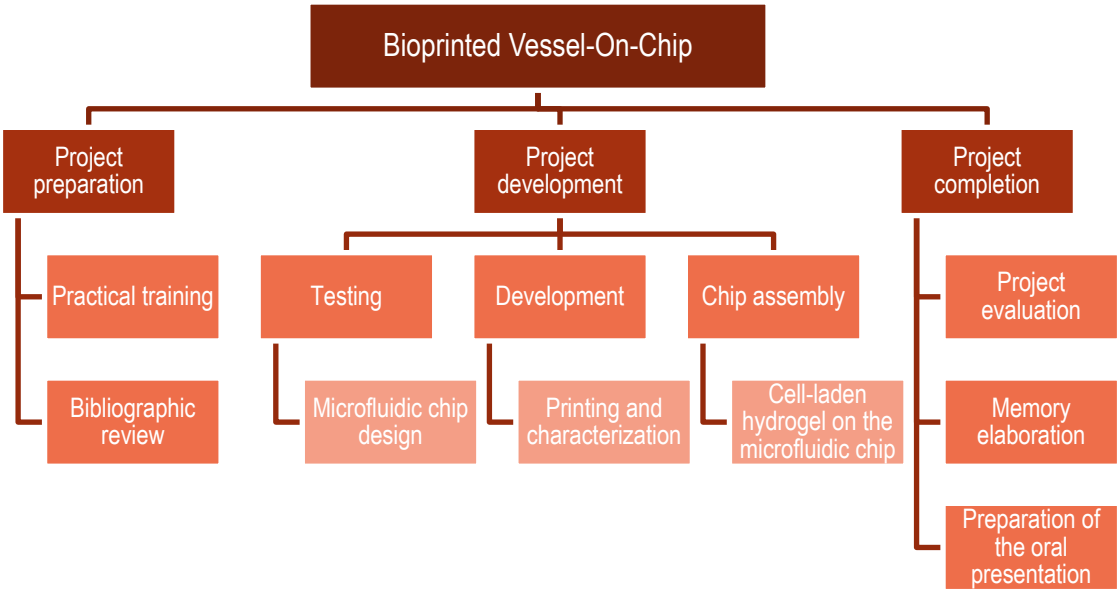

Figure 27: Work Breakdown Structure

6.2. Task definition

Task 1 - Project preparation

1.1 Practical training: Acquire the basic training to use the facilities and equipment in IBEC required for the project. This task also included learning all the basic laboratory tasks: cell culture maintenance, viability tests, among others.

1.2 Bibliographic review: Define the aim and scope of the project as well as studying the state of the art in which the project was developed. This section included the search on how microfluidic devices for OoC applications are developed (materials, technologies, bonding and the microfluidic set-up), how 3D culture can be achieved, and how cells are included in VoC.

Task 2 – Project development

2.1 Testing

2.1.1 Microfluidic chip design: Design, test and validate the different designs for VoC including the analysis on the technology performance, the dimensions, the geometry, the bonding techniques, and the material.

2.2 Development

2.2.1 Printing and characterization: Prepare the bioink to 3D print the hydrogel, which was freshly prepared in every experiment, characterize the hydrogel dimensions for each chip design and perform the 3D printing process in the cleanroom.

2.3 Chip assembly

2.3.1 Cell-laden hydrogel on the microfluidic chip: Assemble the hydrogel with cells embedded in the microfluidic chip and culture them under flow for several days.

Task 3 – Project completion

3.1 Project evaluation: Process and analyze the data after each test and experiment to improve the chip. Conclusions were drawn at the end of the project.

3.2 Memory elaboration: Collect the data and bibliografphy obtained through the entire project.

3.3 Preparation of the oral presentation: Summarize the main points of the project and prepare a clear presentation to discuss results with the jury.

6.3. PERT-CPM

Table 4 shows the tasks involved in the project, order of execution and the duration of each activity.

Table 4: Ordered tasks required to perform the project.

Task	Activity	Description	Previous activities	Following activities	Duration (Weeks)
1.1	A	Practical training	-	C,D	8
1.2	B	Bibliographic review	-	C,G	20
2.1.1	C	Microfluidic chip design	A,B	E	13
2.2.1	D	Printing and characterization	A	E	13
2.3.1	E	Chip assembly	C,D	F	4
3.1	F	Project evaluation	E	G	6
3.2	G	Memory elaboration	B,F	H	5
3.3	H	Oral presentation	G	-	1

From the task planning, PERT-CPM Chart was created (see Figure 28).

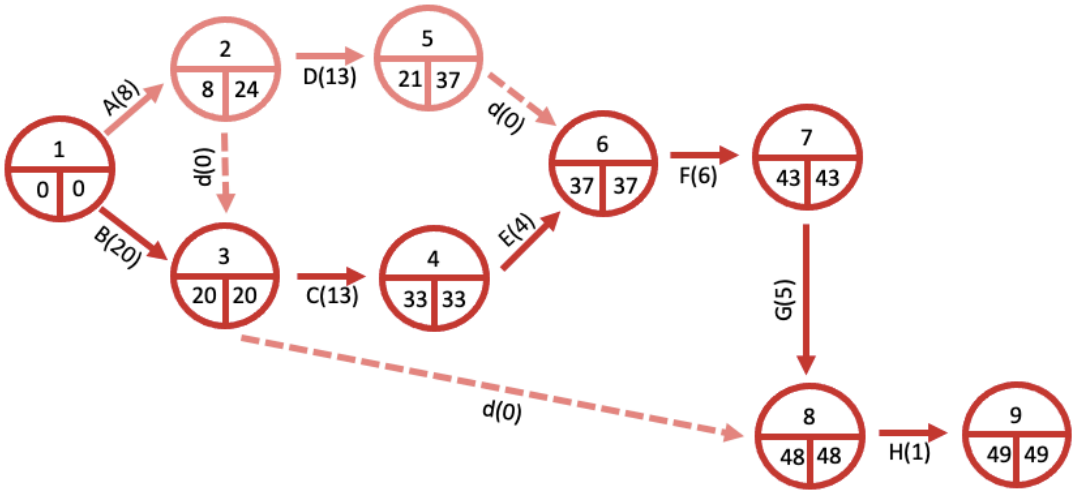

Figure 28: PERT-CPM Chart

6.4. GANTT chart

The project schedule is illustrated in the following GANTT chart.

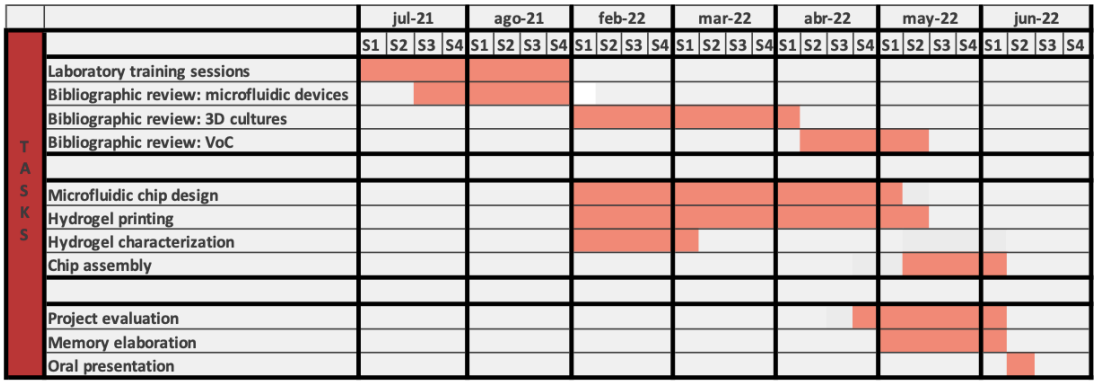

Figure 29: GANTT chart

7. Technical feasibility

Table X shows the analysis on the strength, weaknesses, opportunities, and threats (SWOT) of the project to analyze its technical feasibility.

Table 5: SWOT analysis

	POSITIVE	NEGATIVE
INTERNAL FACTORS	**STRENGHTS** - Mimic the *in vivo* environment - Independent channels - Easy to fabricate - Reusable devices - High resolution and control of the scaffold architecture - Direct microscopy inspection (*in situ* monitoring)	**WEAKNESSES** - Time-consuming bonding technique - Requires the manipulation of the hydrogel that may be responsible for low cell viability in the chip. - Leakage when the screws are not tightened enough. - Require controlled temperature and humidity conditions for bioprinting. - Optical microscope inspection in the laboratory up to 20x.
EXTERNAL FACTORS	**OPPORTUNITIES** - High expectations and demand on the potential of Ooc systems - Increase of areas of application - Integrate sensors	**THREATHS** - No current legislation or validation methods.

8. Economic feasibility

This project has been carried out at the Biomimetics systems for cell engineering group of IBEC, which has provided the equipment, facilities and funds for its development. Some equipment was provided by the Nanobioengineering group and from IBEC Core Facilities. These last ones had an additional cost (see Table 6).

Table 6: Equipment used from IBEC Core Facilities with an additional cost.

EQUIPMENT	HOURS	PRICE RATE(€/H)
OVEN	6	4.44
SOLUS 3D PRINTER	25	16.52
CONFOCAL MICROSCOPY	8	28

Table 7 show the reagents, materials and software used and their corresponding cost.

Table 7: Cost of the reagents, material and software.

	RESOURCE	UNITS	UNITY COST (€)
REAGENTS	Dulbecco's Modified Eagle Medium (DMEM)	500 ml	25.8
	Normocin	600 ul	7.6
	Fetal Bovine Serum (FBS)	125 ml	175
	Trypsin-EDTA	60 ml	10.5
	Pen/Strep	20 ml	10.5
	Phosphate Buffer Saline Solution	1 l	90.5
	Gelatin Porcine skin type A	10 g	2.75
	Methacrytic anhydride	5 ml	0.72
	Polyethylene glycol diacrylate (pegda)	300 mg	64.5
	Lithium phenyl-2,4,6-trimethylbenzoylphosphinate (LAP)	150 mg	20.4
	Tartrazine	2.5 mg	1
	HBSS	10 ml	0.5
	Live/DeadTM viability/cytotoxicity assay kit	15 ul	250
	Hoechst	9 ul	0.2
	PMMA sheets	3	10.65
	PSA	1	37.6
	PDMS pre-polymer elastomer and curing agent	1 kg	173
	PET sheet	1	193
	Mate Gray ABS like Phrozen resin	1 kg	70
MATERIALS	Labware	-	600
	Labcoat	1	25
	Laboratory notebook	1	15
	Teflon tubes ID	1	26.2
	Silicon tubes ID 0.76 mm	1	74
	Silicon two-stop peristaltic pump tubing ID 0.76 mm	1	91
	Screws set M2	1	12.5
	Nuts M2	1	10.5
	Aluminum molds	5	695
SOFTWARE	FreeCAD	-	0
	Fusion 360 *	-	0
	R Studio	-	0
	Microsoft office 365	-	0
	Fiji-ImageJ	-	0
		TOTAL COST	2693.42

*used with Student License.

Therefore, considering the cost of the equipment, products and the supervision and tutoring from an experienced researcher (25€/h) the total expenditure was around 10.000€.

9. Regulations

Currently, there are not specific regulations or standards to develop OoCs, although they are required to facilitate the validation process of OoCs. For this purpose, the European Union (EU) initiated the ORCHID project in 2017, which is also intended to connect all the relevant skateholders in the field. To do so, ORCHID set 5 main objectives including the development of the state of the art of OoCs, the identification of the ethical issues, an analysis on the economic and social impact of the technology, the development of a roadmap to develop these devices and report on the technology to raise awareness. The defined roadmap consists of six steps: initial development, specifications, qualifications, standardization, production and upscaling, adoption and application (Figure 29) [62].

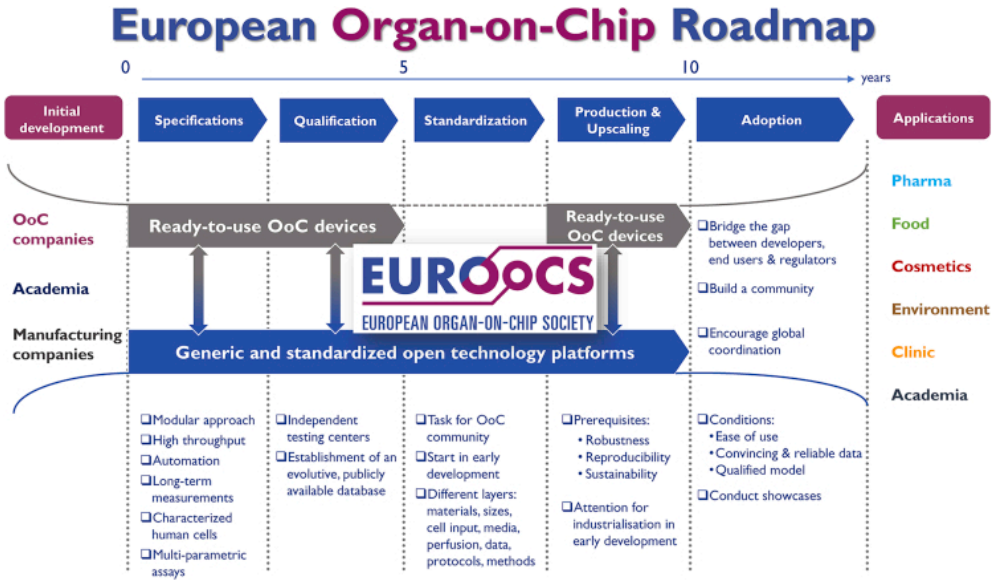

Figure 29: The European OoC Roadmap. From [62].

After the end of the project in 2019, the European Organ-on-Chip Society (EUROoCS) was born. It is an independent non-profit organization established to encourage the OoC research, provide opportunities to share and advance knowledge and expertise in the field [63]. However, a recent PSIS (Putting Science into Standards) workshop suggested a bridging role for EUROoCS for standardization in the OoC roadmap. For OoC qualification, EUROoCS is already encouraging the community to come up with well-documented showcases to catalyze the development of the qualification methodology and infrastructure for OoC [64].

Moreover, on the one hand, since OoC researchers and developers manipulate with biological agents, several regulations must be followed:

- Directive 2004/23/EC of the European Parliament and of the Council of 31 March 2004, which sets the standards of quality and safety for the donation, procurement, testing, processing, preservation, storage and distribution of human tissues and cells.[65]
- Directive 2000/54/EC of the European Parliament and of the Council of 18 September 2000 on the protection of workers from risks related to exposure to biological agents at work. [66]

On the other hand, OoCs are presented to be an alternative to the use of animals in research. In this context, the JRC's European Union Reference Laboratory for alternatives to animal testing (EURL ECVAM) goal is to minimize animal testing for scientific and educational purposes according to the Directive 2010/63/EU. Moreover, they are currently collaborating with the EUROoCS in the implementation of quality control assays carried out by testing centers to evaluate the performance of the in vitro models [67].

10. Conclusions and future work

OoC is an emerging technology that has caught the attention of researchers and pharmaceutical companies because of its promise to better recapitulate the human physiology and thus, increase the reliability of the *in vitro* studies on drug development and toxicology tests. Despite the fact that nowadays OoC developers have been able to create some functional devices that are efficient and effective, there are still some unsolved challenges, as, for example, the use of cell-laden soft materials and their integration to the hard external casing that connects the system to the microfluidic setup.

Therefore, in this project we developed a PMMA-based microfluidic device encasing a cell-laden hydrogel that mimics a blood vessel and its microenvironment. Specifically, we fabricated a 3D bioprinted hydrogel using SLA-DLP technology able to sustain fibroblasts culture within, reproducing the stromal compartment. This hydrogel with embedded cells was then encased inside a microfluidic chip made of patterned PMMA and kept in culture under flouw conditions for several days, maintaining a suitable cell viability.

An adapted hot-embossing technique was used to fabricate the microfluidic chip thanks to the ability of PMMA of being mouldable when reaching the glass transition temperature. This property allowed the transfer of a pattern in a mold to PMMA pieces to create the final architecture of the microfluidic device. The performance of the technology was compared when using resin molds and aluminum molds. Even though aluminum molds are fabricated by an external supplier which yields a high-cost, its heat conductive nature has made them achieve an increase of the resolution of the transfers about 25% and suitable to provide higher reproducibility of the technique than when using 3D printed resin molds.

Nonetheless, since several geometries and dimensions (depending on the requirement to fit the printing support of the hydrogel into the chip, the external casing method used to seal it and the number of channels) were explored to fabricate the final microfluidic device, tests on the designs were done with resin molds because they can be easily obtained in the laboratory with a 3D printer, whereas, aluminum molds were requested to obtain the final microfluidic chip.

A challenge in OoC development is how to seal the device so that enough pressure is applied to avoid leakage ensuring channel independency, without damaging the cells encapsulated in the hydrogel. Two approaches were studied, the first one using a PSA sheet/foil and the second one using screws and a second PMMA layer. The first one allowed for a fast and simple assembly of

the chips and cell viability was very high, but channels were not fully independent (some intercommunications appeared -leakage-). In contrast, the second approach ensured channel independency and avoided leakage, but the method was time-consuming and the percentage of living cells reported was lower. However, this second approach was preferred since it meets the requirements set for the development of a microfluidic device.

To assess the cell viability of the embedded cells, several experiments were performed to confirm the biocompatibility of the materials used and the viability of the device to be used for cell culture. Although obtaining a cell viability of over 50% after 7 days in culture in the chips, which proved its feasibility to be used as an OoC, the obtained values were not as high as expected due to leakage issues, which left some channels without flow, when chips were sealed with PSA. This result encouraged us to adopt the use of screws to seal the devices (second approach), in which, even though leakage was reduced, the results from the cell viability assay were even lower than when using the adhesive sealing approach. This assay should be performed again in the future to verify the setup and the sealing of the device. Once guaranteed, the next step would be to seed the endothelial cells in the laterals of the hydrogels, through the channels of the device, to model the blood vessel, by perfusion of the cell suspension.

Because the model has been assessed in a double-channel device, to increase the complexity and functionality of the model, the triple-channel chip should be reviewed in the future. The assessment will include the hydrogel design test, the cell viability assay, and the endothelial seeding on the middle channel.

Finally, OoC end-users request rapid, easy and precise fabrication and set-up of the devices. Therefore, since the current used technologies are scalable, providing with the appropriate equipment, it would be possible to fabricate multiple devices simultaneously. Moreover, the robustness and predictiveness of the model should be assessed to ensure stable experimental conditions when used in drug screening and toxicology tests. Nonetheless, the biomimetic VoC device might potentially be used to study the course of colorectal cancer and test new therapeutic strategies.

11. Bibliography

[1] L. G. Griffith and M. A. Swartz, “Capturing complex 3D tissue physiology in vitro,” Nature Reviews Molecular Cell Biology 2006 7:3, vol. 7, no. 3, pp. 211–224, Mar. 2006, doi: 10.1038/nrm1858.

[2] M. W. van der Helm, A. D. van der Meer, J. C. T. Eijkel, A. van den Berg, and L. I. Segerink, “Microfluidic organ-on-chip technology for blood-brain barrier research,” https://doi.org/10.1080/21688370.2016.1142493, vol. 4, no. 1, Jan. 2016, doi: 10.1080/21688370.2016.1142493.

[3] D. Vera, M. García-Díaz, N. Torras, M. Álvarez, R. Villa, and E. Martinez, “Engineering Tissue Barrier Models on Hydrogel Microfluidic Platforms,” ACS Applied Materials and Interfaces, vol. 13, no. 12, pp. 13920–13933, 2021, doi: 10.1021/acsami.0c21573.

[4] T. K. Merceron and S. v. Murphy, “Hydrogels for 3D Bioprinting Applications,” Essentials of 3D Biofabrication and Translation, pp. 249–270, Jan. 2015, doi: 10.1016/B978-0-12-800972-7.00014-1.

[5] A. P. Kuo, N. Bhattacharjee, Y. S. Lee, K. Castro, Y. T. Kim, and A. Folch, “High-Precision Stereolithography of Biomicrofluidic Devices,” Adv Mater Technol, vol. 4, no. 6, Jun. 2019, doi: 10.1002/ADMT.201800395.
[6] A. Schwab, R. Levato, M. D’Este, S. Piluso, D. Eglin, and J. Malda, “Printability and Shape Fidelity of Bioinks in 3D Bioprinting,” Chemical Reviews, vol. 120, no. 19, pp. 11028–11055, Oct. 2020, doi: 10.1021/ACS.CHEMREV.0C00084/ASSET/IMAGES/LARGE/CR0C00084_0009.JPEG.
[7] M. L. Coluccio et al., “Microfluidic platforms for cell cultures and investigations,” Microelectronic Engineering, vol. 208, pp. 14–28, Mar. 2019, doi: 10.1016/J.MEE.2019.01.004.
[8] “Microfluidics: A general overview of microfluidics - Elveflow.” https://www.elveflow.com/microfluidic-reviews/general-microfluidics/a-general-overview-of-microfluidics/ (accessed Jun. 05, 2022).
[9] S. N. Bhatia and D. E. Ingber, “Microfluidic organs-on-chips,” Nature Biotechnology 2014 32:8, vol. 32, no. 8, pp. 760–772, Aug. 2014, doi: 10.1038/NBT.2989.
[10] “Colorectal Cancer: Statistics | Cancer.Net.” https://www.cancer.net/cancer-types/colorectal-cancer/statistics (accessed Jun. 05, 2022).
[11] N. del Piccolo et al., “Tumor-on-chip modeling of organ-specific cancer and metastasis,” Advanced Drug Delivery Reviews, vol. 175, p. 113798, Aug. 2021, doi: 10.1016/J.ADDR.2021.05.008.
[12] “Bioengineering against cancer: IBEC researchers receive funding from La Caixa - Institute for Bioengineering of Catalonia.” https://ibecbarcelona.eu/bioengineering-against-cancer-ibec-researchers-receive-funding-from-la-caixa/ (accessed Jun. 05, 2022).
[13] “Blood Vessels and Endothelial Cells - Molecular Biology of the Cell - NCBI Bookshelf.” https://www.ncbi.nlm.nih.gov/books/NBK26848/ (accessed Jun. 05, 2022).
[14] C. Frantz, K. M. Stewart, and V. M. Weaver, “The extracellular matrix at a glance,” Journal of Cell Science, vol. 123, no. 24, p. 4195, Dec. 2010, doi: 10.1242/JCS.023820.
[15] Q. Wu et al., “Organ-on-a-chip: recent breakthroughs and future prospects,” BioMedical Engineering OnLine 2020 19:1, vol. 19, no. 1, pp. 1–19, Feb. 2020, doi: 10.1186/S12938-020-0752-0.
[16] N. Y. Lee, “Recent Progress in Lab-on-a-Chip Technology and Its Potential Application to Clinical Diagnoses,” International Neurourology Journal, vol. 17, no. 1, p. 2, Mar. 2013, doi: 10.5213/INJ.2013.17.1.2.
[17] Q. Meng, Y. Wang, Y. Li, and C. Shen, “Hydrogel microfluidic-based liver-on-a-chip: Mimicking the mass transfer and structural features of liver,” Biotechnology and Bioengineering, vol. 118, no. 2, pp. 612–621, Feb. 2021, doi: 10.1002/BIT.27589.
[18] J. H. Sung and M. L. Shuler, “A micro cell culture analog (microCCA) with 3-D hydrogel culture of multiple cell lines to assess metabolism-dependent cytotoxicity of anti-cancer drugs,” Lab Chip, vol. 9, no. 10, pp. 1385–1394, 2009, doi: 10.1039/B901377F.
[19] P. J. Lee, P. J. Hung, and L. P. Lee, “An artificial liver sinusoid with a microfluidic endothelial-like barrier for primary hepatocyte culture,” Biotechnology and Bioengineering, vol. 97, no. 5, pp. 1340–1346, Aug. 2007, doi: 10.1002/BIT.21360.
[20] O. Kilic et al., “Brain-on-a-chip model enables analysis of human neuronal differentiation and chemotaxis,” Lab on a Chip, vol. 16, no. 21, pp. 4152–4162, Oct. 2016, doi: 10.1039/C6LC00946H.
[21] Y. S. Torisawa et al., “Bone marrow–on–a–chip replicates hematopoietic niche physiology in vitro,” Nature Methods 2014 11:6, vol. 11, no. 6, pp. 663–669, May 2014, doi: 10.1038/NMETH.2938.

[22] “PDMS: a review on polydimethylsiloxane in microfluidics - Elveflow.” https://www.elveflow.com/microfluidic-reviews/general-microfluidics/the-polydimethylsiloxane-pdms-and-microfluidics/ (accessed Jun. 05, 2022).
[23] M. Campisi, Y. Shin, T. Osaki, C. Hajal, V. Chiono, and R. D. Kamm, “3D Self-Organized Microvascular Model of the Human Blood-Brain Barrier with Endothelial Cells, Pericytes and Astrocytes,” Biomaterials, vol. 180, p. 117, Oct. 2018, doi: 10.1016/J.BIOMATERIALS.2018.07.014.
[24] A. Tajeddin and N. Mustafaoglu, “Design and Fabrication of Organ-on-Chips: Promises and Challenges,” Micromachines (Basel), vol. 12, no. 12, Dec. 2021, doi: 10.3390/MI12121443.
[25] E. Roy et al., “Overview of Materials for Microfluidic Applications,” Advances in Microfluidics - New Applications in Biology, Energy, and Materials Sciences, Nov. 2016, doi: 10.5772/65773.
[26] P. M. Kristiansen, A. Karpik, J. Werder, M. Guilherme, and M. Grob, “Thermoplastic Microfluidics,” Methods in Molecular Biology, vol. 2373, pp. 39–55, 2022, doi: 10.1007/978-1-0716-1693-2_3.
[27] S. S. Deshmukh and A. Goswami, “Hot Embossing of polymers – A review,” Materials Today: Proceedings, vol. 26, pp. 405–414, Jan. 2020, doi: 10.1016/J.MATPR.2019.12.067.
[28] “Plastic Injection Moulding, Rapid Prototyping | Protolabs.” https://www.protolabs.co.uk/services/injection-moulding/plastic-injection-moulding/ (accessed Jun. 05, 2022).
[29] P. G. Miller and M. L. Shuler, “Design and demonstration of a pumpless 14 compartment microphysiological system,” Biotechnology and Bioengineering, vol. 113, no. 10, pp. 2213–2227, Oct. 2016, doi: 10.1002/BIT.25989.
[30] F. Akther, P. Little, Z. Li, N. T. Nguyen, and H. T. Ta, “Hydrogels as artificial matrices for cell seeding in microfluidic devices,” RSC Advances, vol. 10, no. 71, pp. 43682–43703, Dec. 2020, doi: 10.1039/D0RA08566A.
[31] L. Li et al., “Three-dimensional hepatocyte culture system for the study of Echinococcus multilocularis larval development,” PLOS Neglected Tropical Diseases, vol. 12, no. 3, p. e0006309, Mar. 2018, doi: 10.1371/JOURNAL.PNTD.0006309.
[32] J. M. Unagolla and A. C. Jayasuriya, “Hydrogel-based 3D bioprinting: A comprehensive review on cell-laden hydrogels, bioink formulations, and future perspectives,” Appl Mater Today, vol. 18, Mar. 2020, doi: 10.1016/J.APMT.2019.100479.
[33] N. Torras, J. Zabalo, E. Abril, A. Carré, M. García-Díaz, and E. Martínez, “A simple DLP-bioprinting strategy produces cell-laden crypt-villous structures for an advanced 3D gut model,” bioRxiv, p. 2022.02.09.479715, Feb. 2022, doi: 10.1101/2022.02.09.479715.
[34] W. Peng, D. Unutmaz, and I. T. Ozbolat, “Bioprinting towards Physiologically Relevant Tissue Models for Pharmaceutics,” Trends in Biotechnology, vol. 34, no. 9, pp. 722–732, Sep. 2016, doi: 10.1016/J.TIBTECH.2016.05.013.
[35] R. Mittal et al., “Organ-on-chip models: Implications in drug discovery and clinical applications,” Journal of Cellular Physiology, vol. 234, no. 6, pp. 8352–8380, Jun. 2019, doi: 10.1002/JCP.27729.
[36] J. Zhang, F. Chen, Z. He, Y. Ma, K. Uchiyama, and J. M. Lin, “A novel approach for precisely controlled multiple cell patterning in microfluidic chips by inkjet printing and the detection of drug metabolism and diffusion,” Analyst, vol. 141, no. 10, pp. 2940–2947, May 2016, doi: 10.1039/C6AN00395H.
[37] S. Naghieh and X. Chen, “Printability–A key issue in extrusion-based bioprinting,” Journal of Pharmaceutical Analysis, vol. 11, no. 5, pp. 564–579, Oct. 2021, doi: 10.1016/J.JPHA.2021.02.001.

[38] W. Liu et al., “Coaxial extrusion bioprinting of 3D microfibrous constructs with cell-favorable gelatin methacryloyl microenvironments,” Biofabrication, vol. 10, no. 2, p. 024102, Jan. 2018, doi: 10.1088/1758-5090/AA9D44.
[39] Q. Gao et al., “3D Bioprinting of Vessel-like Structures with Multilevel Fluidic Channels,” ACS Biomaterials Science and Engineering, vol. 3, no. 3, pp. 399–408, Mar. 2017, doi: 10.1021/ACSBIOMATERIALS.6B00643/SUPPL_FILE/AB6B00643_SI_002.AVI.
[40] D. Hakobyan et al., “Laser-assisted 3D bioprinting of exocrine pancreas spheroid models for cancer initiation study,” Biofabrication, vol. 12, no. 3, p. 035001, Apr. 2020, doi: 10.1088/1758-5090/AB7CB8.
[41] H. Kumar and K. Kim, “Stereolithography 3D Bioprinting,” Methods in Molecular Biology, vol. 2140, pp. 93–108, 2020, doi: 10.1007/978-1-0716-0520-2_6.
[42] R. Zhang and N. B. Larsen, “Stereolithographic hydrogel printing of 3D culture chips with biofunctionalized complex 3D perfusion networks,” Lab on a Chip, vol. 17, no. 24, pp. 4273–4282, Dec. 2017, doi: 10.1039/C7LC00926G.
[43] P. Rajendran et al., “The Vascular Endothelium and Human Diseases,” International Journal of Biological Sciences, vol. 9, no. 10, p. 1057, Nov. 2013, doi: 10.7150/IJBS.7502.
[44] C. J. Mandrycky, C. C. Howard, S. G. Rayner, Y. J. Shin, and Y. Zheng, “Organ-on-a-chip systems for vascular biology,” Journal of Molecular and Cellular Cardiology, vol. 159, pp. 1–13, Oct. 2021, doi: 10.1016/J.YJMCC.2021.06.002.
[45] J. P. Morgan et al., “Formation of microvascular networks in vitro,” Nature Protocols 2013 8:9, vol. 8, no. 9, pp. 1820–1836, Aug. 2013, doi: 10.1038/NPROT.2013.110.
[46] Y. S. Zhang et al., “Bioprinted thrombosis-on-a-chip,” Lab on a Chip, vol. 16, no. 21, pp. 4097–4105, Oct. 2016, doi: 10.1039/C6LC00380J.
[47] S. Kim, H. Lee, M. Chung, and N. L. Jeon, “Engineering of functional, perfusable 3D microvascular networks on a chip,” Lab on a Chip, vol. 13, no. 8, pp. 1489–1500, Mar. 2013, doi: 10.1039/C3LC41320A.
[48] M. Watanabe and R. Sudo, “Microfluidic Device Setting by Coculturing Endothelial Cells and Mesenchymal Stem Cells,” Methods in Molecular Biology, vol. 2206, pp. 57–66, 2021, doi: 10.1007/978-1-0716-0916-3_6/FIGURES/5.
[49] “Organ-on-Chip Market Size & Growth Statistics By 2030.” https://www.alliedmarketresearch.com/organ-on-chip-market (accessed Jun. 05, 2022).
[50] B. Zhang, A. Korolj, B. F. L. Lai, and M. Radisic, “Advances in organ-on-a-chip engineering,” Nature Reviews Materials 2018 3:8, vol. 3, no. 8, pp. 257–278, Aug. 2018, doi: 10.1038/s41578-018-0034-7.
[51] K. Viravaidya, A. Sin, and M. L. Shuler, “Development of a Microscale Cell Culture Analog To Probe Naphthalene Toxicity,” Biotechnology Progress, vol. 20, no. 1, pp. 316–323, Jan. 2004, doi: 10.1021/BP0341996.
[52] R. Li, / Loc, B. Zhang, and M. Radisic, “Organ-on-a-chip devices advance to market,” Lab on a Chip, vol. 17, no. 14, pp. 2395–2420, Jul. 2017, doi: 10.1039/C6LC01554A.
[53] A. D. van der M. , H. P. , J. F. , D. S. , F. T. , D. C. 1 , J. N. 1 , P. N. 1 , S. B. 1 , C. B. 1 , M. Z. 3 , K. K. 1 , D. E. I. 4 , G. A. H. 1 , and M. A. O. 3 . R. Barrile, “Organ-on-Chip Technology Recapitulates Thrombosis Induced by an anti-CD154 Therapeutic Monoclonal Antibody,” 2018, doi: 10.1002/cpt.742.
[54] “OrganoReady® Blood Vessel HUVEC.” https://www.mimetas.com/en/organoready-blood-vessel-huvec/ (accessed Jun. 05, 2022).
[55] A. E. Chen et al., “3D Bioprinted Human Liver Tissue for Modeling Progressive Liver Disease Technology Overview”.

[56] T. Mohamed et al., “Lab-on-a-Printer™-3D Bioprinting Technology Enabling Functional Human Tissues on Demand”.
[57] “3D Bioprinting Market Size & Share Report, 2022 - 2030.” https://www.grandviewresearch.com/industry-analysis/3d-bioprinting-market (accessed Jun. 05, 2022).
[58] A. van den Berg et al., “Microfluidic lab-on-a-chip platforms: requirements, characteristics and applications,” Chemical Society Reviews, vol. 39, no. 3, pp. 1153–1182, Feb. 2010, doi: 10.1039/B820557B.
[59] “Properties of Polmethacrylate.” https://polymerdatabase.com/polymer%20classes/Polymethacrylate%20type.html (accessed Jun. 05, 2022).
[60] “Microfluidic Chip: What is Bonding process in microfluidics?” https://microliquid.com/microfluidic-chips-what-is-bonding/ (accessed Jun. 05, 2022).
[61] T. A. N. Bañuls Díaz Maria, García-Díaz María and Elena Martínez Fraiz, “Final Degree Project Biomedical Engineering - Development of vessel-on-chip,” no. January, 2021.
[62] “ORCHID | organ-on-chip in development.” https://h2020-orchid.eu/ (accessed Jun. 05, 2022).
[63] “Organ-on-Chip – Organ-on-chip digital platform.” https://euroocs.eu/ (accessed Jun. 05, 2022).
[64] M. Mastrangeli and J. van den Eijnden-van Raaij, “Organs-on-chip: The way forward,” Stem Cell Reports, vol. 16, no. 9, p. 2037, Sep. 2021, doi: 10.1016/J.STEMCR.2021.06.015.
[65] “EUR-Lex - 32004L0023 - EN - EUR-Lex.” https://eur-lex.europa.eu/legal-content/EN/TXT/?uri=celex%3A32004L0023 (accessed Jun. 05, 2022).
[66] “Directive 2000/54/EC - biological agents at work | Safety and health at work EU-OSHA.” https://osha.europa.eu/nol/legislation/directives/exposure-to-biological-agents/77 (accessed Jun. 05, 2022).
[67] “Legislation for the protection of animals used for scientific purposes - Environment - European Commission.” https://ec.europa.eu/environment/chemicals/lab_animals/legislation_en.htm (accessed Jun. 05, 2022).
[68] A. D. van der Meer, A. A. Poot, M. H. G. Duits, J. Feijen, and I. Vermes, “Microfluidic technology in vascular research,” Journal of Biomedicine and Biotechnology, vol. 2009, 2009, doi: 10.1155/2009/823148.
[69] D. A. Foyt, M. D. A. Norman, T. T. L. Yu, and E. Gentleman, “Exploiting Advanced Hydrogel Technologies to Address Key Challenges in Regenerative Medicine,” Advanced Healthcare Materials, vol. 7, no. 8, Apr. 2018, doi: 10.1002/ADHM.201700939.